Chapter 18
Sliding Mode Control Design Procedure for Power Electronic Converters Used in Energy Conversion Systems

Yazan M. Alsmadi, Vadim Utkin and Longya Xu

18.1 Introduction

Due to its order reduction property, good dynamic performance and low sensitivity to disturbances and plant parameter variations, sliding mode control (SMC) has been the method of choice for handling nonlinear systems with uncertain dynamics and disturbances. Moreover, this control methodology reduces the complexity of feedback control design since the system is decoupled into independent lower dimensional subsystems [38, 39]. Because of these properties, sliding mode control has a wide range of applications in the areas of electric motors, power systems, power electronics, robotics, aviation and automotive control [1, 38–40].

Power electronic converters belong to the category of circuits controlled by switching devices with "ON/OFF" as the only admissible operating states [22, 28]. Therefore, control variables can take only values from a discrete set. For this type of circuits, SMC is preferred not only from a theoretical view but also a technological one. In the past, State Space Averaging approach was the method of choice to analyze some of the power conversion circuits [26, 35]. Using this technique, state space models and equations are obtained for each possible switch's position. The equations are then averaged over a switching cycle to obtain a low frequency averaged model. Linear

Y.M. Alsmadi (✉)
Department of Electrical Engineering, Jordan University of Science and Technology, Irbid 22110, Jordan
e-mail: ymalsmadi@just.edu.jo

V. Utkin · L. Xu
Department of Electrical and Computer Engineering, The Ohio State University, Columbus, OH 43212, USA
e-mail: utkin.2@osu.edu

L. Xu
e-mail: xu.12@osu.edu

J.B. Clempner and W. Yu (eds.), *New Perspectives and Applications of Modern Control Theory*, https://doi.org/10.1007/978-3-319-62464-8_18

(after linearization if needed) or nonlinear control theory are then applied to design a feedback compensator. SMC provides a powerful tool to control power converters such that linearization is not needed and analysis and control design methods are developed in the framework of the nonlinear models [26, 33, 35, 39].

The main drawback of any system with pulse-width modulation (PWM) control approaches, including SMC, is the appearance of undesirable oscillations having finite amplitude and frequency due to the presence of unmodeled dynamics or discrete time implementation. This phenomenon, called "Ripple" in power electronics literature or "Chattering" in control theory, may lower control accuracy or incur unwanted wear of mechanical components [24, 39, 40]. An additional obstruction of SMC is the fact that it results in frequency variations, which is not acceptable in many applications [24].

Although the methods outlined in literature [4, 9, 10, 12–14, 36] showed efficient suppression of chattering, these methods are disadvantageous or not even applicable when dealing with power electronics systems controlled by switches with "ON/OFF" as the only admissible operating states. For example, gain-dependent and equivalent-control based methods are not applicable to reduce chattering since the output of power converters can only take two (or finite number of) values. Equivalent control method of SMC also yields the continuous motion equation directly. This motion, called "slow motion," exits along with high frequency components [40]. The boundary layer approach, on the other hand, avoids generating sliding mode by replacing the discontinuous control action with a continuous saturation function [36, 38–40]. However, control discontinuities are inherent to these power electronics systems. When implementing a continuous controller, techniques such as PWM have to be exploited to adopt the continuous control law and feed it to the discontinuous system inputs. Therefore, it seems unjustified to bypass the inherent discontinuities in the system by converting a continuous control law to a discontinuous one by means of PWM. As an alternative, discontinuous control inputs should be used directly in control, and new methods should be investigated to reduce chattering under these operating conditions [38–40].

The most natural and straightforward way to reduce chattering in power converters is to increase the switching frequency. As technology progresses, switching devices are manufactured with enhanced switching frequency (up to 100 s KHz) and high power rating. However, heat power losses enforce a new restriction. Even though switching is possible with high switching frequency; it is limited to the maximum allowable heat losses caused by switching.

The objective of this chapter is to provide a comprehensive sliding mode control design procedure for power electronic converters that are used in energy conversion systems. This includes the DC/DC, AC/DC and DC/AC power electronic converters.

First, a comprehensive control design procedure for DC/DC power converters based on sliding mode control methodology. The input inductor current control and subsequently output capacitor voltage regulation for different types of DC/DC are investigated. Sliding mode control algorithms for Buck and Boost converters with incomplete information about system states are developed by designing state

observers. Chattering issues are also discussed and a chattering reduction design approach for power converters is proposed.

Second, a new sliding model control strategy for AC/DC power converters is presented. The basic idea is to apply a feedback implementation of Pulsewidth Modulation (PWM). The proposed control algorithm exhibits low sensitivity to disturbances and fast dynamic performance in addition to the main converter properties. This includes unity power factor, sinusoidal input currents, and low level of DC output voltage ripple.

Third, Sliding Mode Pulsewidth Modulation (SMPWM) control methodologies for current-controlled inverters are proposed. Two novel approaches based on the sliding mode concept are presented to make the system tracking reference inputs. The proposed approaches control the phase currents and the neutral point voltage simultaneously. Optimization of different operational criteria is also presented.

18.2 Sliding Mode Control of DC/DC Power Converters

The input inductor current and the output capacitor voltage are normally selected as state variables for DC/DC converters. For most converters used in practice, the motion rate of the current is much faster than the motion rate of the output voltage. Calling upon the Singular Perturbation theory [19, 20],[1] the control problems of the DC/DC converters can be solved by using a cascaded control structure with two control loops: an inner current loop and an outer voltage loop. The current control loop is based on PWM that can be implemented using SMC or hysteresis control while output voltage regulation is normally a result of the current control loop such that output voltage converges to the desired reference value if designing the ideal current tracking system is accomplished [32, 34, 39].

18.2.1 Direct SMC of DC/DC Power Converters

(A) Buck-Type DC/DC Converters

The circuit structure of a Buck-type DC/DC converter is shown in Fig. 18.1, where E is the source voltage, C is the storage capacitor, L is the loop inductor, R is the load resistance, I is the input current and V is the output voltage.

Based on circuit analysis, the dynamic model of the Buck converter is given by:

$$\dot{x}_1 = -\frac{1}{L}x_2 + u\frac{E}{L} \tag{18.1}$$

[1]Formally, conventional Singular Perturbation Theory is not applicable for differential equations with discontinuous right-hand side. But, if sliding mode appears, sliding mode equations are in compliance with the conditions of the theory.

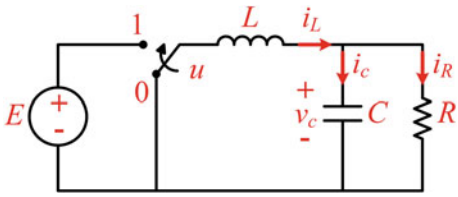

Fig. 18.1 Buck-type DC/DC converter

$$\dot{x}_2 = -\frac{1}{C}x_1 + \frac{1}{RC}x_2 \tag{18.2}$$

where $x_1 = I$ and $x_2 = V$.

The switching function of the switch can be defined as:

$$u = \begin{cases} 1 & switch\ is\ closed \\ 0 & switch\ is\ open \end{cases} \tag{18.3}$$

The control objective is to achieve a constant output voltage denoted by V_d. In other words, the steady state behavior of the Buck converter should be given by:

$$x_2 = V_d \tag{18.4}$$

$$\dot{x}_2 = \dot{V}_d = 0 \tag{18.5}$$

The proposed design methodology follows a two-step procedure known as integrator backstepping or regular form control [23, 25, 43]. First, it is assumed that x_1 in Eq. (18.2) can be handled as a control input. However, since x_1 is also the output of the current loop, given by Eq. (18.1), this first design step leads to the desired current $x^*{}_1$. After substituting Eqs. (18.4) and (18.5) into (18.2), the desired current is given by:

$$x^*{}_1 = \frac{V_d}{R} \tag{18.6}$$

The goal of the second step of the proposed design procedure is to ensure that the actual current x_1 tracks the desired current $x^*{}_1$ exactly. Due to its ideal tracking properties, sliding mode approach is an efficient tool for this task. If sliding mode is enforced in:

$$s = x_1 - x^*{}_1 = 0 \tag{18.7}$$

then, $x_1 = V_d/R$. In order to enforce sliding mode in the manifold $s = 0$, control u is defined as:

$$u = \frac{1}{2}\left(1 - sign\,(s)\right) \tag{18.8}$$

The condition for sliding mode to exist is derived from ($\lim_{t\to+0} \dot{s} < 0$, $\lim_{t\to-0} \dot{s} > 0$). As a result, sliding mode is enforced if:

$$0 < x_2 < E \tag{18.9}$$

Equation (18.9) defines an attraction domain of the sliding manifold. Since the control u, given by Eq. (18.8), does not contain a control gain that needs to be adjusted, the domain of attraction, given by Eq. (18.9) is predetermined by the system architecture. In steady state conditions, Eq. (18.9) is fulfilled by the definition of a Buck converter where the output voltage is smaller than the source voltage.

After the state of the inner current loop has reached the sliding manifold, i.e. converged to $s = 0$ at time $t = t_h$, $x_1 = x^*{}_1 = V_d/R$ holds for $t > t_h$ and the outer voltage loop is governed by:

$$\dot{x}_2 = -\frac{1}{RC}x_2 + \frac{1}{RC}V_d \tag{18.10}$$

The solution of Eq. (18.10) is given by:

$$x_2 = V_d + (x_2\,(t_h) - V_d)\; e^{\frac{-1}{RC}(1-t_h)} \tag{18.11}$$

where x_2 tends to V_d exponentially. Hence, the goal of the proposed control design is achieved.

(B) Boost-Type DC/DC Converters

The circuit structure of a Boost-type DC/DC converter is shown in Fig. 18.2, where circuit variables are similar to those defined for the Buck converter. Based on circuit analysis, the dynamic model of the Boost converter is given by:

$$\dot{x}_1 = -\,(1-u)\,\frac{1}{L}x_2 + \frac{E}{L} \tag{18.12}$$

$$\dot{x}_2 = (1-u)\,\frac{1}{C}x_1 - \frac{1}{RC}x_2 \tag{18.13}$$

where $x_1 = I$ and $x_2 = V$ and switching function u is given by Eq. (18.3).

Boost converters are more difficult to control than Buck converters. This is because of the fact that the control u appears in the voltage and current equations, and both in a bilinear fashion. Such a configuration implies a highly nonlinear system with

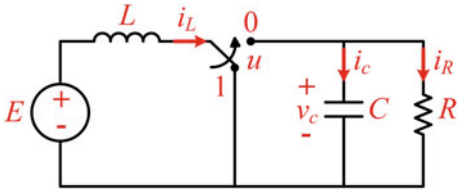

Fig. 18.2 Boost-type DC/DC converter

a difficult control design. It also leads to unstable dynamics with respect to current when voltage is the only variable to be controlled [32, 34].

Since Boost converters satisfy the Motion-Separation principle that is based on the *Singular Perturbation theory* [19, 20], their control problems can also be solved by using two cascaded control loops: an inner current and an outer voltage control loops. Sliding Mode control techniques will be used again to design the current control loop.

Similar to the proposed control design for the Buck converter, the desired current is obtained from the outer voltage loop as:

$$x^*{}_1 = \frac{{V_d}^2}{RE} \tag{18.14}$$

where V_d is the desired output capacitor voltage. The switching function of the inner current control is defined as:

$$s = x_1 - x^*{}_1 \tag{18.15}$$

In order to enforce the current x_1 to track the desired current $x^*{}_1$, control u can be designed as:

$$u = \frac{1}{2}\left(1 - sign\left(s\right)\right) \tag{18.16}$$

Under the above control scheme, the equivalent control is formally derived by substituting $\dot{s} = \dot{x_1} = 0$ in (18.12) and solve for the control input u as:

$$u_{eq} = 1 - \frac{E}{x_2} \tag{18.17}$$

where x_2 is the output voltage of the slow voltage loop. The motion equation of the outer voltage loop during sliding mode is obtained by substituting the equivalent control, given by Eq. (18.17), into (18.13).

$$\dot{x}_2 = -\frac{1}{RC}\left(x_2 - \frac{{V_d}^2}{x_2}\right) \tag{18.18}$$

Equation (18.18) can be solved explicitly as:

$$x_2 = \sqrt{{V_d}^2 + \left({x_2}^2\left(t_h\right) - {V_d}^2\right)\, e^{\frac{-2}{RC}\left(t - t_h\right)}} \tag{18.19}$$

where t_h represents the reaching instant of the sliding manifold $s = 0$ and $x_2\left(t_h\right)$ is the output voltage at time t_h. Apparently, x_2 tends to V_d asymptotically as time goes to infinity.

The attraction domain of the sliding manifold $s = 0$ is found by applying the convergence condition $s\dot{s} < 0$ to the Eqs. (18.12) and (18.13), yielding:

$$x_2 > E \text{ or } 0 < u_{eq} = 1 - \frac{E}{x_2} < 1 \tag{18.20}$$

Condition (18.20) implies that sliding mode can be enforced as long as the output voltage is higher than the source voltage. This requirement is essential for a Boost-type DC/DC converter. A careful consideration of the initial conditions is also required to guarantee the convergence to $s = 0$.

18.2.2 Observer-Based Sliding Mode Control of DC/DC Converters

In recent years, research on sliding mode control theory has revealed great advantages of incorporating certain dynamics into the sliding mode controllers [38–40]. This new approach, called *Observer-based Sliding Mode Control*, fall into the category of dynamic feedback control where the sliding mode controller simulates the ideal plant model in parallel with the real one [25, 38, 42]. This helps to reduce the number of states that need to be measured since the real plant states are substituted by observer states. The mismatch between the measurable state(s) and the observed one is the 'bridge' that establishes coupling between the plant system space and the controller space and keeps both systems operating close to each other. It can also be been utilized in different ways to improve the control performance. Overall, an observer can be viewed as an artificially introduced auxiliary dynamic system in order to improve the control performance [11, 16].

This subsection investigates the input inductor current control and subsequently output capacitor voltage regulation for different types of DC/DC. It develops sliding mode control algorithms for Buck and Boost converters with incomplete information about system states by designing state observers. For Buck converters governed by linear equations, conventional observer design methods could be applied directly while non-linear observers should be designed for Boost converters. It is assumed that the variable under control is measured only for both converters.

(A) Observer-Based Control of Buck-Type DC/DC Converters

The observer equations, or the auxiliary system, of the buck converter are designed as:

$$\widehat{\dot{x}}_1 = -\frac{1}{L}\hat{x}_2 + u\frac{E}{L} - l_1\left(\hat{x}_1 - x_1\right) \tag{18.21}$$

$$\widehat{\dot{x}}_2 = \frac{1}{C}\hat{x}_1 - \frac{1}{RC}\hat{x}_2 - l_2\left(\hat{x}_1 - x_1\right) \tag{18.22}$$

where l_1, l_2 are constant scalar observer gains and $\hat{x}_1$, $\hat{x}_2$ are the estimates of the inductor current and output voltage. Note that it is only required to measure the inductor current x_1.

Equations with respect to the mismatches $\overline{x}_1$, $\overline{x}_2$ are defined as:

$$\overline{x}_1 = \hat{x}_1 - x_1 \tag{18.23}$$

$$\overline{x}_2 = \hat{x}_2 - x_2 \tag{18.24}$$

The error dynamics can be derived by subtracting Eqs. (18.1) and (18.2) from (18.21) and (18.22):

$$\dot{\overline{x}}_1 = -\frac{1}{L}\overline{x}_2 - l_1\overline{x}_1 \tag{18.25}$$

$$\dot{\overline{x}}_2 = \frac{1}{C}\overline{x}_1 - \frac{1}{RC}\overline{x}_2 - l_2\overline{x}_1 \tag{18.26}$$

The characteristic polynomial of the above linear system is defined as:

$$P^2 + \left(l_1 - \frac{1}{RC}\right)P + \left(-\frac{l_1}{RC} - \frac{1}{LC} - \frac{l_2}{L}\right) = 0 \tag{18.27}$$

For the second order error system given in Eq. (18.27), stability and desired rate of convergence can be provided by the proper choice of l_1, l_2. This implies that the observer errors $\overline{x}_1$ and $\overline{x}_2$ tend to zero asymptotically.

The switching function for the sliding mode current controller will be designed based on the observed current $\hat{x}_1$ instead of the measured current x_1 as done in Eq. (18.7):

$$\hat{s} = \hat{x}_1 - \frac{V_d}{R} \tag{18.28}$$

The control u that is applied to the real plant and the observer system is of the same form as in the case of the control scheme without an observer.

$$u = \frac{1}{2}\left(1 - sign\left(\hat{s}\right)\right) \tag{18.29}$$

Assuming that sliding mode can be enforced in the vicinity of the sliding manifold $\hat{s} = 0$, $\hat{x}_1$can be calculated as:

$$\hat{x}_1 \equiv \frac{V_d}{R}\ with\ \forall t > t_h \tag{18.30}$$

where t_h denotes the reaching instant of the sliding manifold $\hat{s}$. The equivalent control of u can be obtained by solving $\dot{\hat{s}} = 0$ with respect to control:

$$u_{eq} = \hat{x}_2\left(\frac{1}{L}\hat{x}_2 - l_1\left(\hat{x}_1 - x_1\right)\right)\frac{L}{E} \tag{18.31}$$

After substituting u_{eq} into the real plant model, given by Eqs. (18.1) and (18.2), and considering the observer model, given by Eqs. (18.21) and (18.22), the motion in sliding mode can be represented as a reduced order system, comprising the motion of the real plant and the slow dynamics (output voltage loop) of the observer, as shown in the following equations:

$$\dot{x}_1 = -\frac{1}{L}\overline{x_2} + l_1\left(\frac{V_d}{R} - x_1\right) \tag{18.32}$$

$$\dot{x}_2 = \frac{1}{C}x_1 - \frac{1}{RC}x_2 \tag{18.33}$$

$$\dot{\hat{x}}_2 = \frac{1}{C}\frac{V_d}{R} - \frac{1}{RC}\hat{x}_2 - l_2\left(\hat{x}_1 - x_1\right) \tag{18.34}$$

Further analysis of Eqs. (18.32)–(18.34) results in:

$$\lim_{t\to\infty} x_1(t) = \hat{x}_1(t)\big|_{t\geq t_h} = \frac{V_d}{R} \tag{18.35}$$

$$\lim_{t\to\infty} x_2(t) = \lim_{n\to\infty} \hat{x}_1(t) = V_d \tag{18.36}$$

The remaining task is to find the condition under which the occurrence of the sliding mode can be guaranteed. Applying the existence condition of sliding mode to Eq. (18.21) along with the substitution of Eqs. (18.28) and (18.29) yields:

$$-Ll_1\left(\hat{x}_1 - x_1\right) < \hat{x}_2 < E - Ll_1(\hat{x}_1 - x_1) \tag{18.37}$$

$$0 < u_{eq} = \left(\frac{1}{L}\hat{x}_2 + l_1\left(\hat{x}_1 - x_1\right)\right)\frac{L}{E} < 1 \tag{18.38}$$

Since $s(0) = 0$ with zero initial conditions for the power converter and E is high enough, sliding mode existence condition (18.38) is fulfilled.

(B) Observer-Based Control of Boost-Type DC/DC Converters

In order to simplify the derivation of the observer-based control scheme of Boost converters, a new control input is introduced and defined as $v = (1 - u)$. The observer dynamics that are designed for a Boost converter are governed by:

$$\dot{\hat{x}}_1 = -v\frac{1}{L}\hat{x}_2 + \frac{E}{L} - l_1\left(\hat{x}_1 - x_1\right) \tag{18.39}$$

$$\dot{\hat{x}}_2 = v\frac{1}{C}\hat{x}_1 - \frac{1}{RC}\hat{x}_2 - l_2\left(\hat{x}_1 - x_1\right) \tag{18.40}$$

where $\hat{x}_1, \hat{x}_2$ are the observed inductor current and output voltage, i.e. outputs of the observer; and l_1, l_2 are positive scalar observer gains.

Equations with respect to the mismatches $\overline{x}_1$, $\overline{x}_2$ are defined as:

$$\overline{x}_1 = \hat{x}_1 - x_1 \tag{18.41}$$

$$\overline{x}_2 = \hat{x}_2 - x_2 \tag{18.42}$$

The error dynamics can be derived by subtracting Eqs. (18.12) and (18.13) from (18.41) and (18.42):

$$\dot{\overline{x}}_1 = -v\frac{1}{L}\overline{x}_2 - l_1\overline{x}_1 \tag{18.43}$$

$$\dot{\overline{x}}_2 = v\frac{1}{C}\overline{x}_1 - \frac{1}{RC}\overline{x}_2 - l_2\overline{x}_1 \tag{18.44}$$

Equations (18.43) and (18.44) are nonlinear, since the system states are multiplied by the control input v. For the convergence proof, select a *Lyapunov* function candidate as:

$$V = \frac{1}{2}(L\overline{x}_1^2 + C\overline{x}_2^2) > 0 \tag{18.45}$$

The time derivative $\dot{V}$ on the system trajectory can be easily calculated as:

$$\dot{V} = -Ll_1\overline{x}_1^2 - \frac{1}{R}\overline{x}_2^2 - Cl_2\overline{x}_1\overline{x}_2 \tag{18.46}$$

Therefore, the convergence rate can be selected can be selected by proper choice of l_1, l_2 under Sylvester condition $\left(\frac{Ll_1}{R} > \frac{(Cl_2)^2}{4}\right)$ for quadratic form (18.46). As a result, observer errors $\overline{x}_1$ and $\overline{x}_2$ tend to zero asymptotically. The convergence rate of the inductor current estimation can be adjusted by the observer gains l_1, l_2.

The switching function of the sliding mode current controller will be designed based on the observed current $\hat{x}_1$ instead of measured current x_1 as done in (18.15):

$$\hat{s} = \hat{x}_1 - \frac{V_d^2}{RE} \tag{18.47}$$

The control u that is applied to the real plant and the observer system is of the same form as in the case of the control scheme without an observer.

$$u = \frac{1}{2}\left(1 - sign\left(\hat{s}\right)\right) \tag{18.48}$$

Equation (18.48) can be represented in terms of the new control input $v = (1 - u)$ as:

$$v = \frac{1}{2}\left(1 - sign\left(\hat{s}\right)\right) \tag{18.49}$$

Assuming that sliding mode can be enforced in the vicinity of the sliding manifold $\hat{s} = 0$, $\hat{x}_1$can be calculated as:

$$\hat{x}_1 \equiv \frac{V_d^2}{RE} \; with \; \forall t > t_h \tag{18.50}$$

where t_h denotes the reaching instant of the sliding manifold $\hat{s}$. The equivalent control of u can be obtained by solving $\dot{\hat{s}} = 0$:

$$v_{eq} = \frac{E - Ll_1(\frac{V_d^2}{RE} - x_1)}{\hat{x}_2} \tag{18.51}$$

After substituting v_{eq} into the real plant model, given by Eqs. (18.12) and (18.13), and considering the observer model, given by Eqs. (18.39) and (18.40), the motion in sliding mode can be represented as a reduced order system, comprising the motion of the real plant and the slow dynamics (output voltage loop) of the observer.

$$\dot{x}_1 = -v_{eq}\frac{1}{L}x_2 + \frac{E}{L} \tag{18.52}$$

$$\dot{x}_2 = v_{eq}\frac{1}{C}x_1 - \frac{1}{RC}x_2 \tag{18.53}$$

$$\dot{\hat{x}}_2 = v_{eq}\frac{1}{C}\frac{V_d^2}{RE} - \frac{1}{RC}\hat{x}_2 - l_2\left(\frac{V_d^2}{RE} - x_1\right) \tag{18.54}$$

By defining the errors $\overline{x}_1^* = \frac{V_d^2}{RE} - x_1$ and $\overline{x}_2 = \hat{x}_2 - x_2$ and since $\overline{x}_1$ tends to zero at the desired rate, the above equations can be transformed into a second order error system as:

$$\dot{\overline{x}}_1^* = -\frac{x_2}{\hat{x}_2}l_1\overline{x}_1^* + \frac{E}{L}\frac{x_2}{\hat{x}_2} - \frac{E}{L} \tag{18.55}$$

$$\dot{\overline{x}}_2 = \frac{E}{C}\frac{1}{\hat{x}_2}\overline{x}_1^* - \frac{Ll_1}{C\hat{x}_2}(\overline{x}_1^*)^2 - \frac{1}{RC}\overline{x}_2 - l_2\overline{x}_1^* \tag{18.56}$$

Further analysis of Eqs. (18.55) and (18.56) results in:

$$\lim_{t\to\infty} \hat{x}_2 = x_2 \tag{18.57}$$

$$\lim_{t\to\infty}\left(\frac{E}{L}\frac{x_2}{\hat{x}_2} - \frac{E}{L}\right) = 0 \tag{18.58}$$

This means that $\overline{x}_1^*$ converges to zero asymptotically at a rate that depends on l_1. As a result, $\overline{x}_2$ and x_2 tend respectively to zero and V_d. The remaining task is to find the condition under which the occurrence of the sliding mode can be

guaranteed. Applying the existence condition of sliding mode to (18.47) along with the substitution of Eqs. (18.39), (18.40) and (18.49) yields:

$$0 < E - Ll_1\left(\hat{x}_1 - x_1\right) < \hat{x}_2 \tag{18.59}$$

$$0 < v_{eq} = \frac{E - Ll_1(\hat{x}_1 - x_1)}{\hat{x}_2} < 1 \tag{18.60}$$

Equation (18.60) can be represented in terms of the new control input $v = (1 - u)$ as:

$$0 < u_{eq} < 1 \tag{18.61}$$

Since x_1 is measured and $\hat{x}_1$, $\hat{x}_2$ are state variables in the controller space, the initial conditions of the observer, $\hat{x}_1(0)$ and $\hat{x}_2(0)$, can be designed such that the occurrence of the sliding mode is always guaranteed.

18.2.3 Simulation Results

In order to evaluate the proposed sliding mode control strategies for DC/DC power converters, several computer simulations have been conducted using MATLAB/Simulink software.

(A) Direct Sliding Mode Control of Boost Converters

Parameters of the simulated Buck converter are listed in Table 18.1. Figures 18.3 and 18.4 show the simulation results of the proposed control algorithm for Boost converters. As it can be seen from the figures, both the inductor current and the output capacitor voltage converge rapidly to their reference values.

(B) Direct Sliding Mode Control of Boost Converters

Parameters of the simulated Boost converter are listed in Table 18.2. Figures 18.5 and 18.6 show the simulation results of the proposed control algorithm for Boost converters. As it can be seen from the figures, both the inductor current and the output capacitor voltage converge rapidly to their reference values.

(C) Observer-Based Sliding Mode Control of Buck Converters

Parameters of the simulated Buck converter are listed in Table 18.1. The observer gain is selected as $l = 200$. Two sets of the observer initial conditions, listed in Table 18.3, were selected in order to compare the influence of observer initial conditions on the system response.

Table 18.1 Simulation parameters of the Buck-type DC/DC converter

Parameter	L (mH)	C (μf)	V_d (V)	R (Ω)	E (V)
Value	40	4	7	40	20

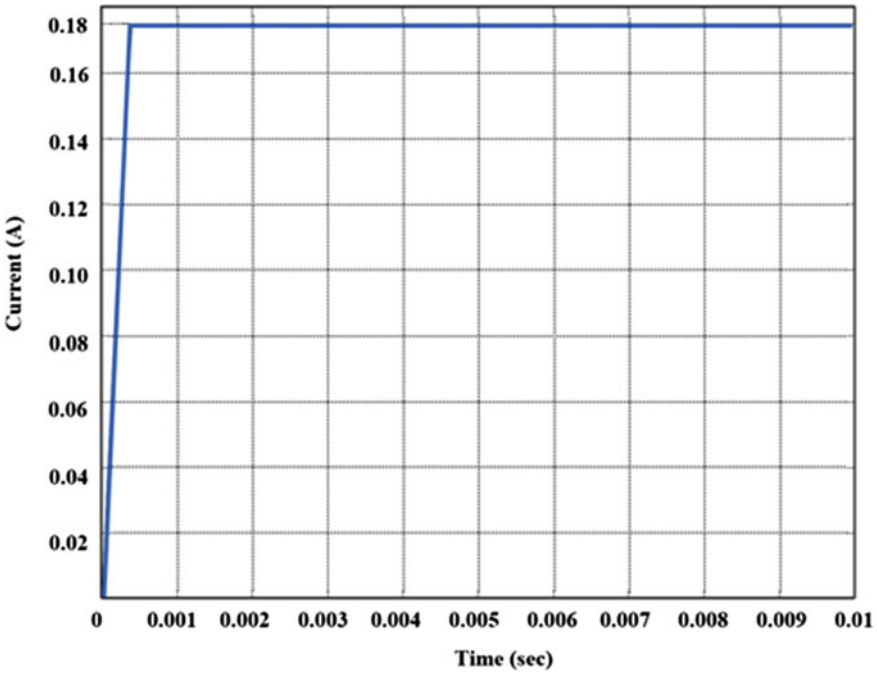

Fig. 18.3 Current response of a sliding mode-controlled Buck DC/DC power converter

Figures 18.7 and 18.8 show the response of real and estimated inductor current and output capacitor voltage under different initial conditions. Note that both the inductor current and the output capacitor voltage converge rapidly to their reference values and the system response can be influenced by the design of the observer initial conditions.

(D) Observer-Based Sliding Mode Control of Boost Converters

Parameters of the simulated Boost converter are listed in Table 18.2. The observer gain is selected as $l = 200$. Two sets of the observer initial conditions, listed in Table 18.4, were selected in order to compare the influence of observer initial conditions on the system response.

Figures 18.9 and 18.10 show the response of real and estimated inductor current and output capacitor voltage under different initial conditions. Note that both the inductor current and the output capacitor voltage converge rapidly to their reference values and the system response can be influenced by the design of the observer initial conditions.

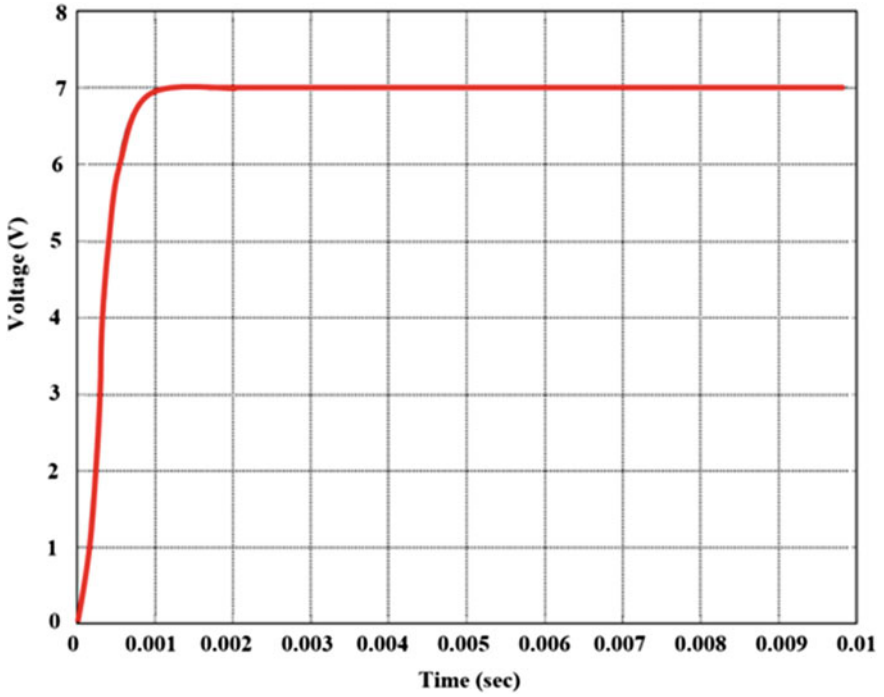

Fig. 18.4 Voltage response of a sliding mode-controlled Buck DC/DC power converter

Table 18.2 Simulation parameters of the Boost-type DC/DC converter

Parameter	L (mH)	C (μf)	V_d (V)	R (Ω)	E (V)
Value	40	4	40	40	20

18.2.4 Sliding Mode Control of Multi-phase DC/DC Power Converters

This section presents a new chattering reduction approach for power converters. The proposed scheme is based on the idea of designing a multi-phase converter system that operates at a given and fixed switching frequency without any additional dynamic elements. This may be possible by providing a desired phase shift between phases for any loads or frequencies in order to implement the "*Harmonic Cancellation*" method [24]. Several attempts have been made to apply this idea to PWM such that phase shifts are interconnected and can be controlled using a transformer with primary and secondary coils in different phases. On the other hand, the phase shift was obtained using delays, filters, or set of triangular inputs with selected delays [27, 45, 48].

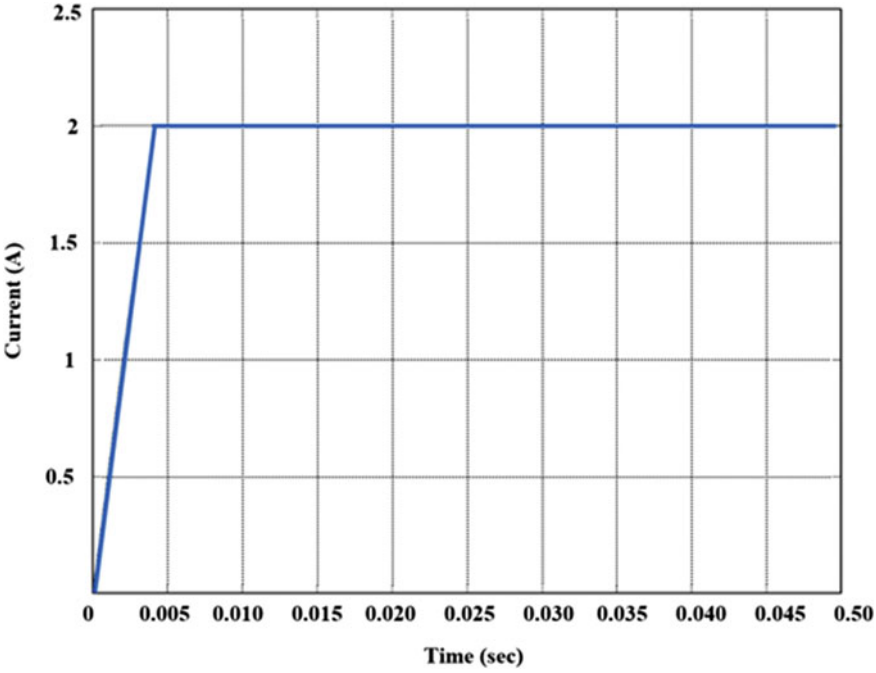

Fig. 18.5 Current response of a sliding mode-controlled Boost DC/DC power converter

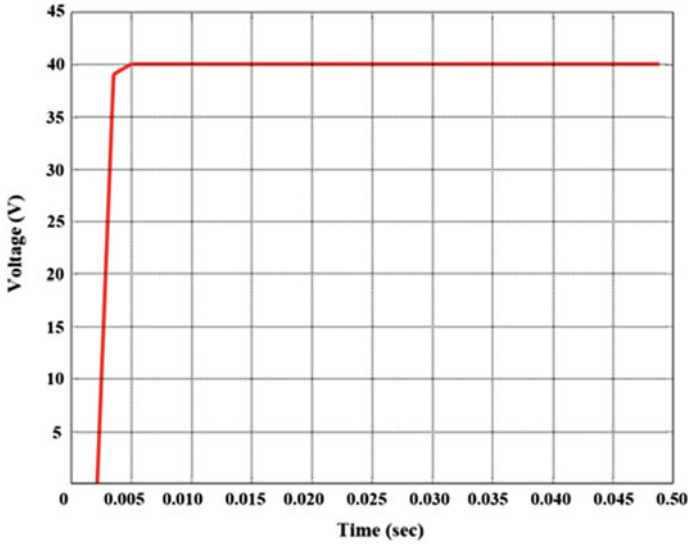

Fig. 18.6 Voltage response of a sliding mode-controlled Boost DC/DC power converter

Table 18.3 Observer initial conditions for the simulated Buck-type DC/DC converter

Initial condition	$\hat{x}_1$ (0) (A)	$\hat{x}_2$ (0) (V)
Set #1	0.12	5
Set #2	0.07	2.5

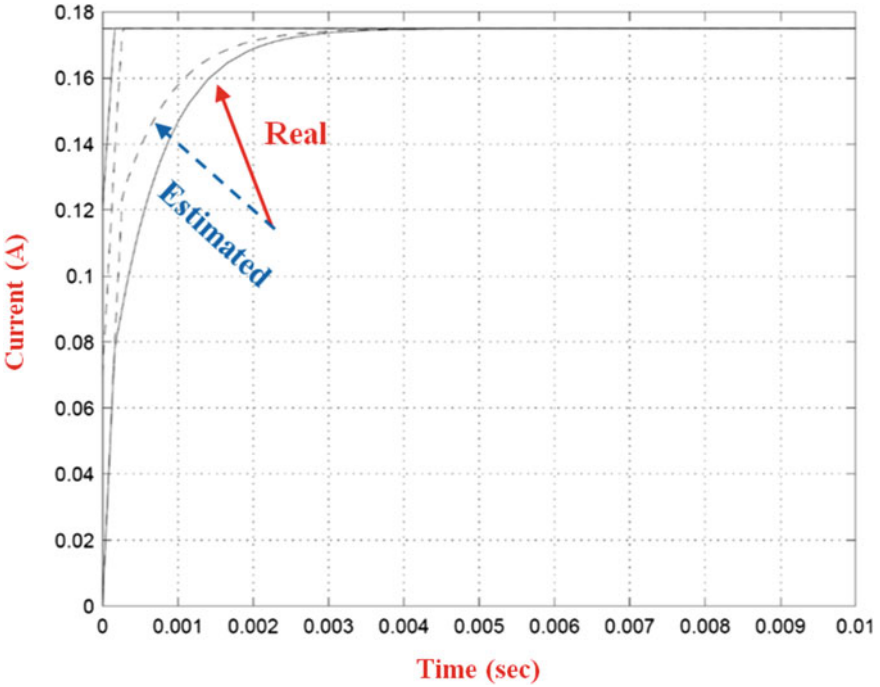

Fig. 18.7 Response of real (curves start from zero) and estimated current of a buck converter under different initial conditions. *Solid line* $\hat{x}_1\,(0) = 0.12$, $\hat{x}_2\,(0) = 5.0$; *dashed line* $\hat{x}_1\,(0) = 0.07$, $\hat{x}_2\,(0) = 2.5$

18.2.4.1 Frequency Control

Chattering frequency normally depends on the width of the hysteresis loop in the switching element which is usually selected such that the frequency does not exceed the maximum admissible level f_{des} for all operation modes. This can be achieved by varying the width of hysteresis loop [9, 29].

It order to formulate the problem statement, the following system with scalar control is considered.

$$\dot{x} = f\,(x,t) + b\,(x,t)\,u \qquad (x,\, f, b \in \mathcal{R}^n) \tag{18.62}$$

It is assumed that control u should be designed as a continuous function of state variables $(u_0\,(x))$. This situation is usually assumed with the "*Cascade Con-*

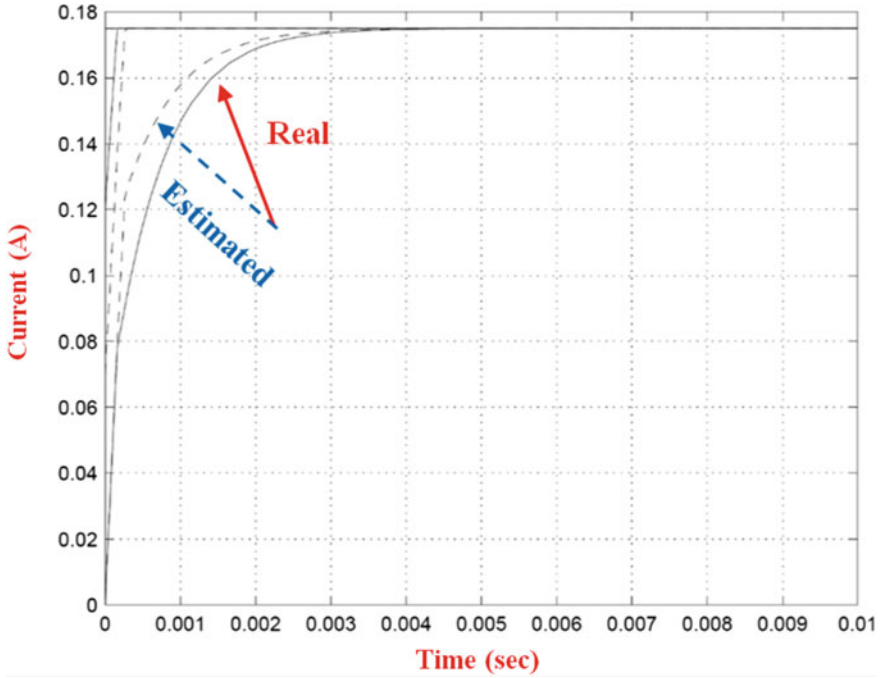

Fig. 18.8 Response of real (curves start from zero) and estimated voltage of a buck converter under different initial conditions. *Solid line* $\hat{x}_1(0) = 0.12$, $\hat{x}_2(0) = 5.0$; *dashed line* $\hat{x}_1(0) = 0.07$, $\hat{x}_2(0) = 2.5$

Table 18.4 Observer initial conditions for the simulated Boost-type DC/DC converter

Initial condition	$\hat{x}_1(0)$ (A)	$\hat{x}_2(0)$ (V)
Set #1	0	0
Set #2	1.95	38.5

trol" approach that is used for electric motors with the current as a control input [23, 39]. Power converters often utilize PWM as a principle operation mode in order to implement the desired control algorithm [22, 28]. Sliding mode is one of the tools to implement this operation mode based on the feedback approach as shown in Fig. 18.11, which illustrates that output u tracks the reference input $u_0(x)$ in sliding mode.

Select the sliding surface as:

$$s = u_0(x) - u,\ \dot{u} = v = Msign(s),\ M > 0 \tag{18.63}$$

$$\dot{s} = g(x) - Msign(s),\ g(x) = [grad(u_0)]^T (f + bu) \tag{18.64}$$

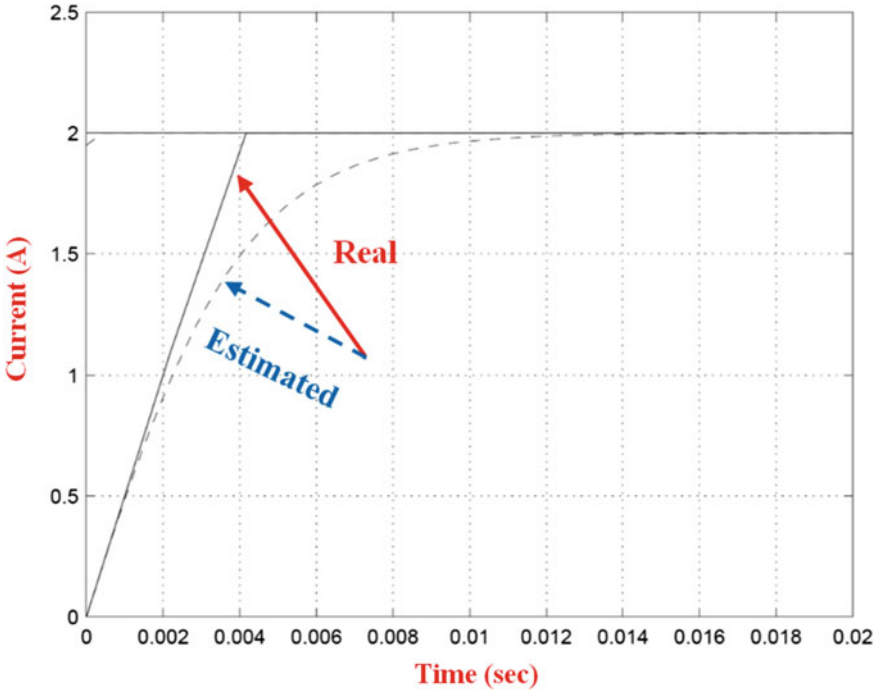

Fig. 18.9 Response of real (curves start from zero) and estimated current of a Boost converter under different initial conditions. *Solid line* $\hat{x}_1\,(0) = 0, \hat{x}_2\,(0) = 0$; *dashed line* $\hat{x}_1\,(0) = 1.95, \hat{x}_2\,(0) = 38.5$

It is evident that sliding mode, in the surface $s = 0$ with $u \equiv u_0$, exists if $M > |g(x)|$. If the control is implemented with a hysteresis loop, the switching frequency can be maintained at the desired level f_{des} by varying the width of the hysteresis loop Δ [24].

$$\Delta = \frac{M^2 - g\,(x)^2}{2M} \frac{1}{f_{des}} \tag{18.65}$$

18.2.4.2 Chattering Suppression

Suppose that the desired control is implemented by m power converters with $s_i = \frac{u_0}{m} - u_i$, $(i = 1, 2, \ldots m)$ and $\frac{u_0}{m}$ as reference inputs as shown in Fig. 18.12. If each power converter operates properly, the output is equal to the desired control $u_0(x)$. Amplitude and frequency of chattering in each converter can be found as:

$$A = \frac{\Delta}{2}, \; f = \frac{M^2 - \left(\frac{g(x)}{m}\right)^2}{2M\Delta} \tag{18.66}$$

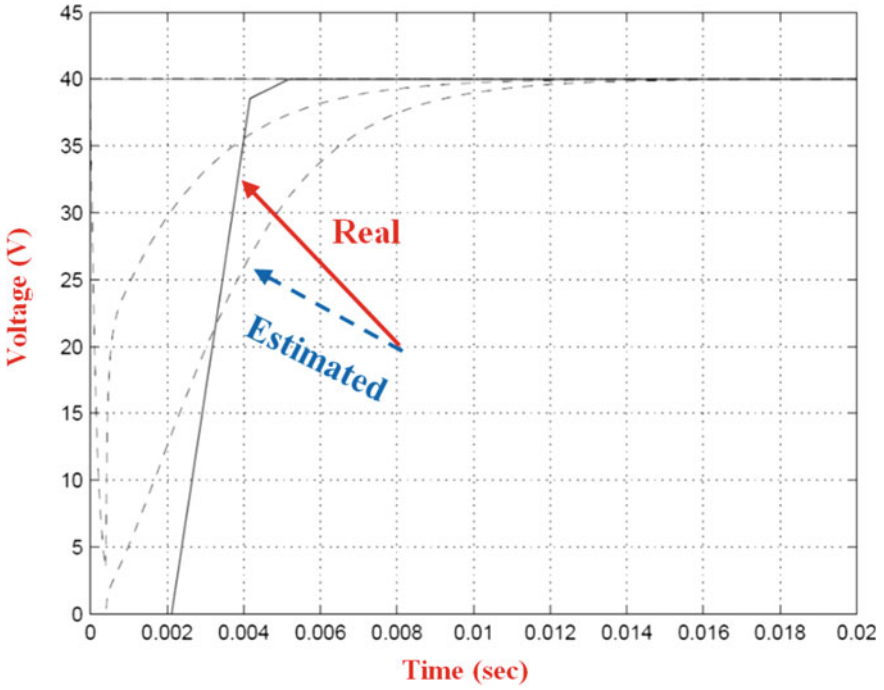

Fig. 18.10 Response of real (curves start from zero) and estimated voltage of a Boost converter under different initial conditions. *Solid line* $\hat{x}_1(0) = 0$, $\hat{x}_2(0) = 0$; *dashed line* $\hat{x}_1(0) = 1.95$, $\hat{x}_2(0) = 38.5$

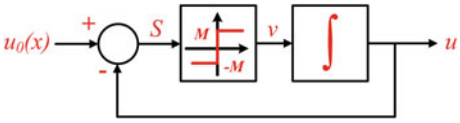

Fig. 18.11 Sliding mode control for a simple power converter model structure

The chattering amplitude of output u depends on the oscillation in each phase. Its maximum value is m times higher than that of each converter. For the system shown in Fig. 18.12, phases depend on initial conditions and cannot be controlled.

First, it should be demonstrated that, by varying phases, the output oscillation amplitude can be controlled. Suppose that a multiphase converter with m phases is to be designed such that the period of chattering T is the same in each phase, and two subsequent phases have phase shift T/m. Since chattering is a periodic time function, it can be represented as Fourier series with frequencies:

$$\omega_k = \omega.k, \omega = \frac{2\pi}{T} \ (k = 1.2 \ldots . \infty) \tag{18.67}$$

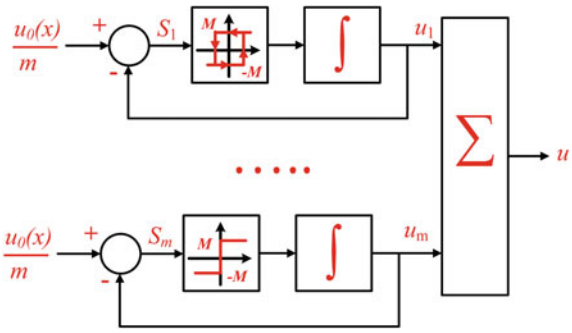

Fig. 18.12 *m*-phase converter with evenly distributed reference

The effect of the k-th harmonic in the output signal is the sum of individual outputs from all phases and can be easily calculated as:

$$\begin{aligned} \sum_{i=0}^{m-1} \sin\left(\omega_k\left(t-\frac{2\pi}{\omega m}i\right)\right) &= \sum_{i=0}^{m-1} Im[e^{j\omega_k t-\frac{2\pi k}{m}i}] \\ &= Im\left(e^{j\omega_k t}Z\right), Z = \sum_{i=0}^{m-1} e^{-j\frac{2\pi k}{m}i} \end{aligned} \tag{18.68}$$

To find Z, consider the following equation:

$$Ze^{-j\frac{2\pi k}{m}} = \sum_{i=0}^{m-1} e^{-j\frac{2\pi k}{m}(i+1)} = \sum_{i'=0}^{m-1} e^{-j\frac{2\pi k}{m}i'} \tag{18.69}$$

Since

$$Ze^{-j\frac{2\pi k}{m}}\Big|_{i=m} = e^{-j\frac{2\pi k}{m}i}\Big|_{i=0} \tag{18.70}$$

then,

$$Ze^{-j\frac{2\pi k}{m}} = Z \tag{18.71}$$

The function $e^{-j\frac{2\pi k}{m}}$ is equal to 1 only if k/m is an integer or $k = m, 2m, \ldots$, which means that $Z = 0$ for all other cases.

The above analysis shows that all harmonics except for lm ($l = 1, 2, \ldots$) are suppressed in the output signal. As a result, the amplitude of chattering can be reduced to the desired level by increasing the number of phases and providing a desired phase shift between each two subsequent phases.

18.2.4.3 Design Principle

In order to describe the design idea of the proposed chattering suppression approach, suppose that two power converters are implemented as shown in Fig. 18.13.

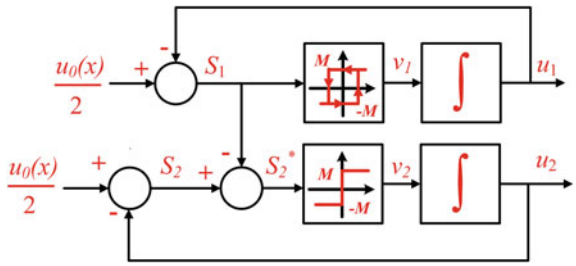

Fig. 18.13 A controller model with two interconnected phases

The switching function for the second converter is selected as:

$$s_2^* = s_2 - s_1 \tag{18.72}$$

where,

$$s_1 = u_0/2 - u_1 \tag{18.73}$$

$$s_2 = \frac{u_0}{2} - u_2 \tag{18.74}$$

$$v_1 = Msign(s_1) v_2 = Msign(s_2^*) \tag{18.75}$$

The time derivatives of s_1, s_2^* are:

$$\dot{s}_1 = a - Msign\,(s_1) \qquad \left(a = \frac{g\,(x)}{2}\right) \tag{18.76}$$

$$\dot{s_2^*} = Msign\,(s_1) - Msign\,(s_2) \tag{18.77}$$

Figures 18.14 and 18.15 analyze the system behavior in the plane s_1 and s_2^* with $a = 0$, $\propto = 1$. Δ and α are the widths of the hysteresis loops for the two sliding surfaces. T can be easily calculated as:

$$T = \frac{\Delta}{M - a} + \frac{\Delta}{M + a} = \frac{2M\Delta}{M^2 - a^2} \tag{18.78}$$

By analyzing Fig. 18.14, it can be seen that the phase shift becomes:

$$\Phi = \frac{\alpha\Delta}{2M} \tag{18.79}$$

where Φ is equal to the time for changing s_2^* from $\frac{\alpha\Delta}{2}$ to $-\frac{\alpha\Delta}{2}$ or vice versa.

The previous analysis demonstrates that the phase shift between oscillations can be selected by proper choice of $\propto$ for any switching frequency without using dynamic elements. The value $\propto$ is calculated to provide the desired phase shift. Since Φ must be equal to *T/m,* $\propto$can be found as:

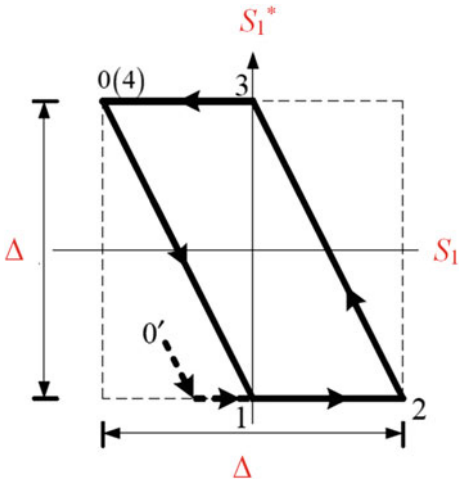

Fig. 18.14 The system behavior in s-plane

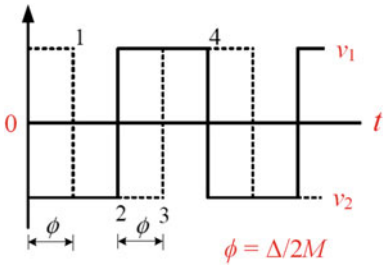

Fig. 18.15 Control of the phase between v_1, v_2

$$\propto = \frac{4M^2}{m(M^2 - a^2)} \tag{18.80}$$

For $a > 0$, $\propto$ can be selected such that phase shift is equal to what we need. Finally, the proposed chattering suppression design procedure for multiphase converters can be summarized as follows:

1. Select the width of the hysteresis loop as a state function such that the switching frequency in the first phase is maintained at the desired level.
2. Determine the number of phases for a given range of α variation.
3. Find the parameter $\propto$ as a function of α such that the phase shift between two subsequent phases is equal to $\frac{1}{m}$ of the oscillation period of the first phase.

Finally, another approach, called "master-slave" method of multiphase converters can be used for chattering reduction even if for a given number of phases m, parameter a is beyond the admissible domain and the desired phase shift cannot be guaranteed by varying the width of the hysteresis loop. For the master-slave implementation, each phase can be complimented by several sequentially connected "slaves", as illustrated

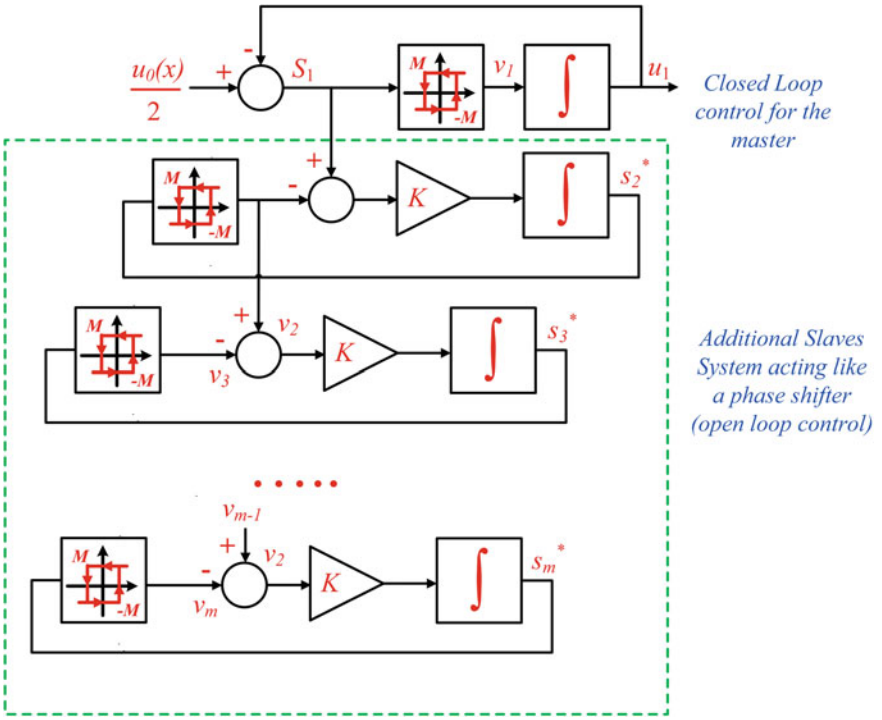

Fig. 18.16 A modified master-slave mode schematic with two more additional systems. $v_{2,3}$ is the switching command for the second channel

in Fig. 18.16 for a two-phase converter, such that the total phase shift is equal to the desired value.

18.2.4.4 Simulation Results

In order to evaluate the proposed sliding mode chattering suppression control strategies for multi-phase DC/DC power converters, computer simulations have been conducted using MATLAB/Simulink software.

Multi-phase DC/DC Converter Topology

The chattering suppression approach developed in the previous section is applied to DC/DC multi-phase buck converters. The objective is to demonstrate, via simulations, the effectiveness of the proposed design methodology in multiphase power converters. Simulations also check the range of the function "***a***" for which the chattering suppression takes place. The "*master-slave*" method is utilized in all simulations. A two-phase DC/DC converter is shown in Fig. 18.17. Simulation parameters are listed in Table 18.5.

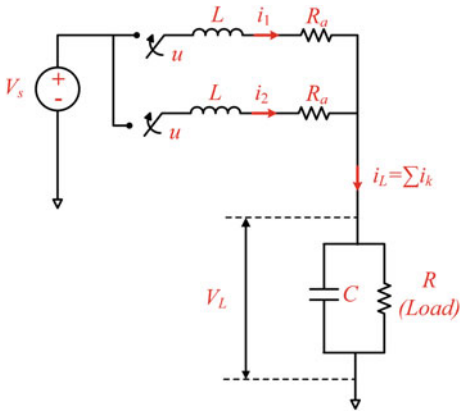

Fig. 18.17 A two-phase DC/DC converter

Table 18.5 Simulation parameters of the two-phase DC/DC converter

Parameter	L (H)	C (F)	R_a (Ω)	R_L (Ω)	V_s (V)
Value	$5 * 10^{-8}$	$1 * 10^{-3}$	$3 * 10^{-4}$	$1 * 10^{-2}$	12

For simulation purposes, the governing equations of the m-phase converter are assumed as follows:

$$\dot{I}_k = \frac{1}{L}(-I_k R_a + u_k - V_L),\ k = 1, 2, \ldots, m \tag{18.81}$$

$$V_L = \frac{1}{C}\left(\sum_{k=1}^{m} I_k - \frac{V_L}{R_L}\right) \tag{18.82}$$

The following control law is used for the two-phase power converter ($m = 2$) represented in Eqs. (18.81) and (18.82):

$$s_1 = I_1 - \frac{I_{ref}}{m},\ I_{ref} = \frac{V_{ref}}{R_L} \tag{18.83}$$

$$u_1 = V_s\left(\frac{1 - sign\,(s_1)}{2}\right) \tag{18.84}$$

$$u_2 = V_s\left(\frac{1 - sign\,(s_3^*)}{2}\right) \tag{18.85}$$

$$\dot{s}_1 = \frac{1}{L}\left(-R_a s_1 - \frac{V_s}{2} sign\,(s_1)\right) + \left(\frac{V_s}{2} - \frac{I_{ref} R_a}{m} - V_L\right) = -M sign\,(s_1) - b s_1 + a \tag{18.86}$$

$$\dot{s}_2^* = M\left(sign\left(s_1\right) - sign\left(s_2^*\right)\right) \tag{18.87}$$

$$\dot{s}_3^* = M\left(sign\left(s_2^*\right) - sign\left(s_3^*\right)\right) \tag{18.88}$$

where V_{ref} and I_{ref} are the reference input voltage and the corresponding reference load current, respectively. $a = \frac{V_s}{2} - \frac{I_{ref}R_a}{m} - V_L$, $M = \frac{V_s}{2L}$ and $b = \frac{R_a}{L}$. The desired phase shift $T/2$ is obtained by using two additional blocks with a phase shift of $T/4$ in each of them. The four-phase converter ($M = 4$) is simulated with switching frequency control of the first phase by appropriate choice of hysteresis width or hysteresis loop gain K_h in order to maintain the switching frequency at 50 Hz. The selected function $K_h\left(V_{ref}\right) = -0.0013V_{ref}^2 + 0.0127V_{ref} - 0.0007$ is shown in Fig. 18.18.

Figures 18.19, 18.20 and 18.21 demonstrates the effectiveness of the proposed chattering suppression algorithm on a 4-phase DC/DC power converter with three different reference inputs, $v_{ref1} = 3\,\text{V}$, $v_{ref2} = 6\,\text{V}$, and $v_{ref3} = 8\,\text{V}$, respectively. Note that the inductance is relatively small in order to have fast converter dynamics. This leads to a high level of chattering in each phase, but it is practically suppressed in the output signal.

Finally, it is demonstrated that chattering can be reduced considerably following the "master-slave method" even if for a given number of phases m, parameter a is beyond the admissible domain and the desired phase shift cannot be guaranteed by

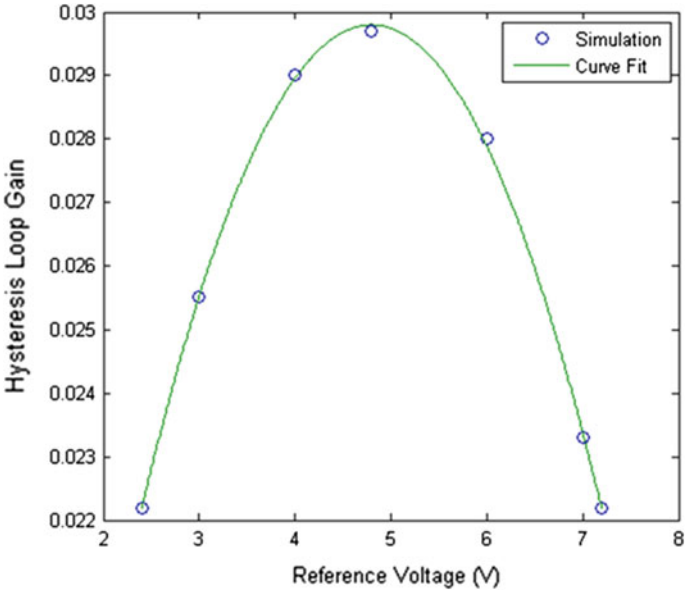

Fig. 18.18 Hysteresis loop gain K_h

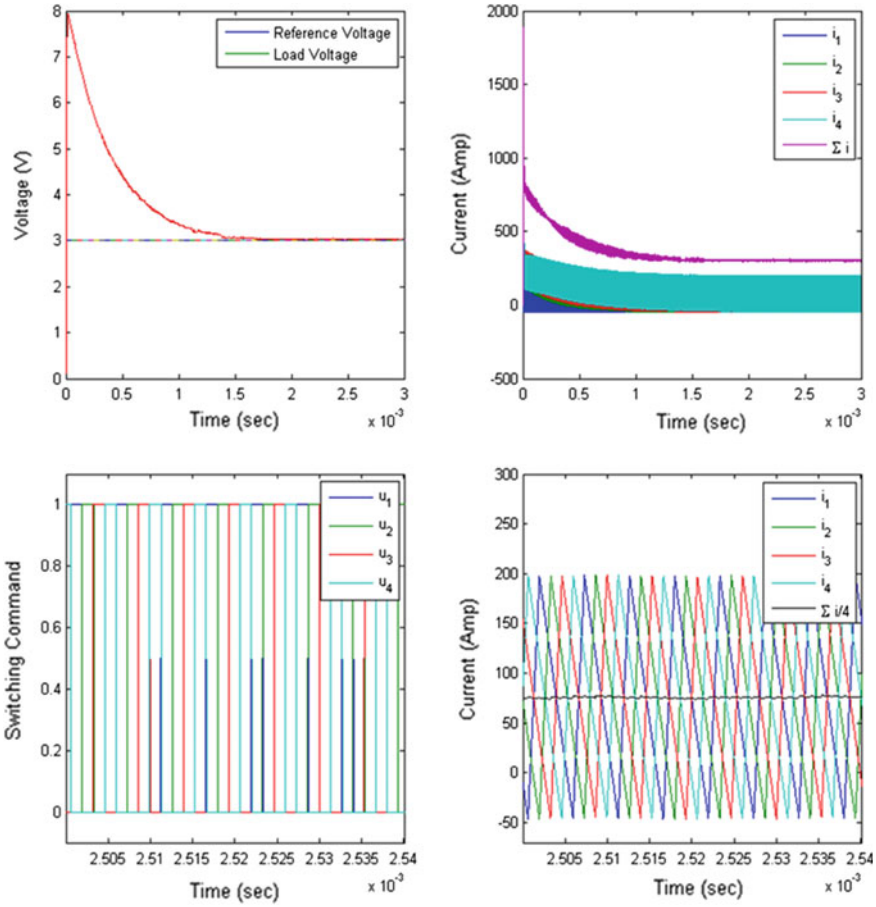

Fig. 18.19 Simulation results for the four-phase DC/DC converter, $V_{ref} = 3\,\text{V}$

varying the width of the hysteresis loop. For the master-slave implementation, each phase can be complimented by several sequentially connected "slaves", as illustrated in Fig. 18.16 for two-phase converter, such that the total phase shift is equal to the desired value. Of course, chattering can be suppressed by increasing the number of phases preserving the "*one slave in one phase*" approach, as shown in Fig. 18.22 for an 8-phase converter.

18.2.4.5 Experimental Results

Experimental results were conducted and discussed in [2] in order to demonstrate the effectiveness of the proposed sliding mode chattering suppression approach for multi-phase converters and also verify the simulation results.

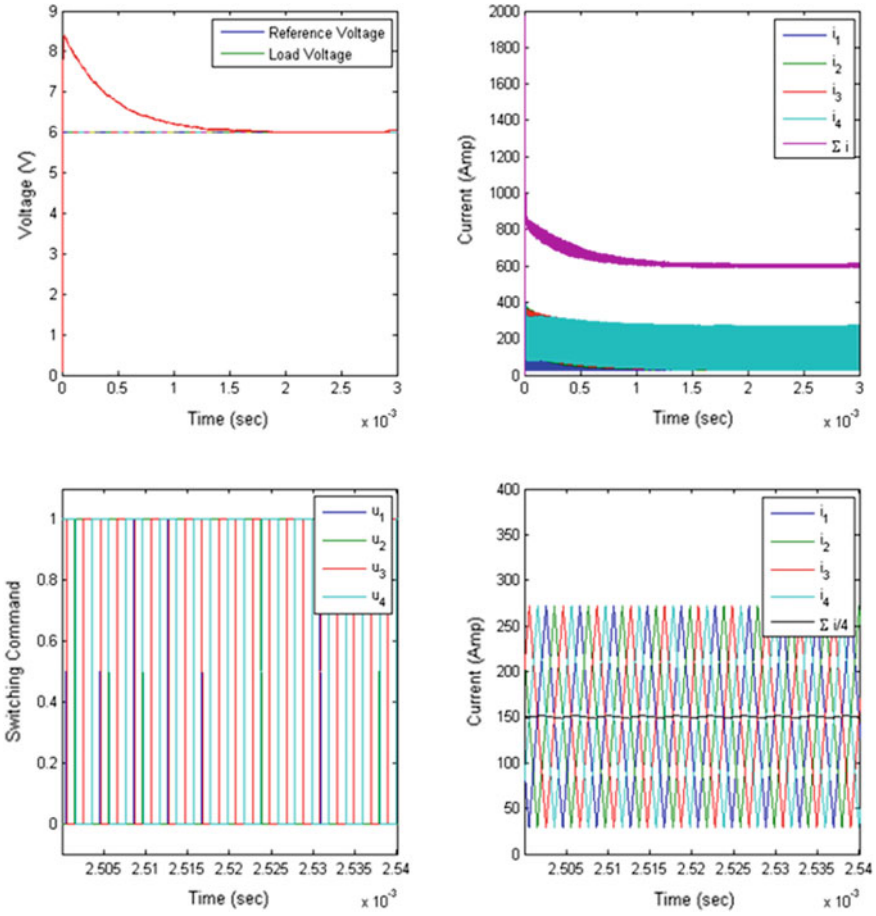

Fig. 18.20 Simulation results for the four-phase DC/DC converter, $V_{ref} = 6\,\text{V}$

Figure 18.23 shows the experimental setup. The system consists of a 4-phase DC/DC buck converter that is controlled using two loops: A current inner loop that is sliding mode controlled with a hysteresis band, and a voltage outer loop that defines the current reference through a PI controller. Table 18.6 shows the converter parameters.

Figure 18.24 shows the experimental waveforms of the input current, output voltage and control command for a half- bridge, 1-phase DC/DC converter. The reference output voltage is 5 V. The average input current value is 2.44 A and the chattering amplitude is 0.47 A. The average output voltage is 4.96 V.

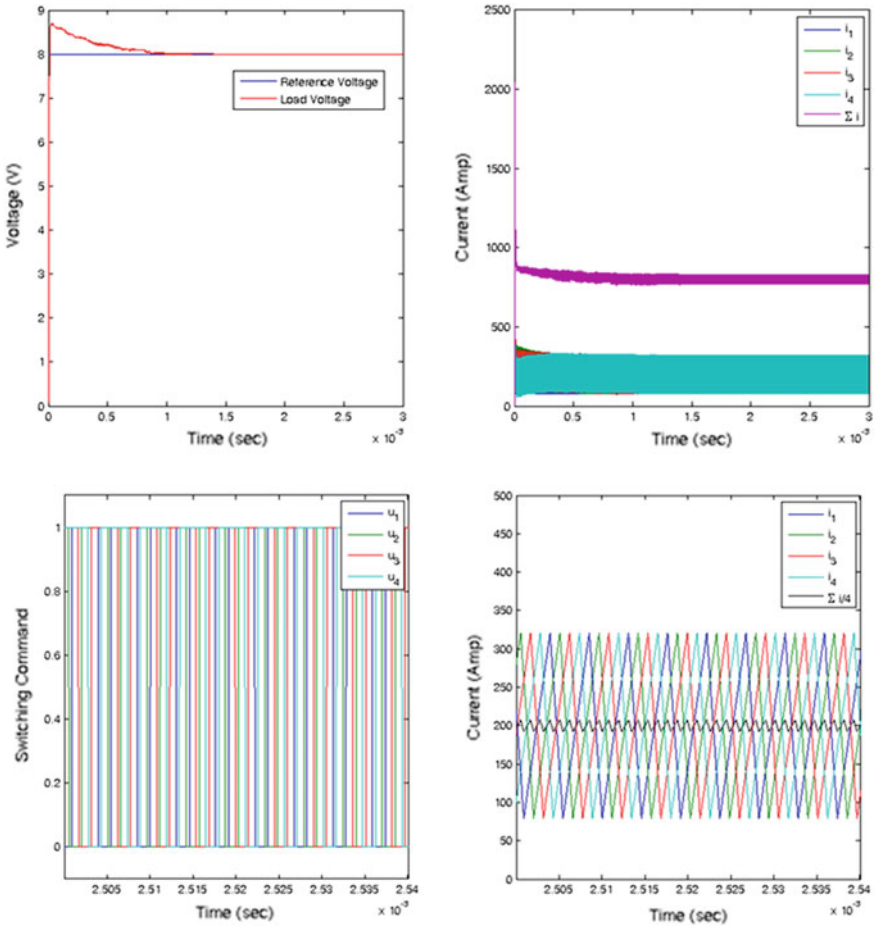

Fig. 18.21 Simulation results for the four-phase DC/DC converter, $V_{ref} = 8\,\text{V}$

Figures 18.25 and 18.26 show the four shifted input currents and the MOSFET drain voltages of a 4-phases DC/DC converter, respectively. Both Figures demonstrate that the master-slave algorithm works properly, with respect to the current shifting. The current values of each phase are $i_{L1} = 0.62 \mp 0.43\,\text{A}$, $i_{L2} = 0.6 \mp 0.42\,\text{A}$, $i_{L3} = 0.63 \mp 0.43\,\text{A}$, and $i_{L4} = 0.66 \mp 0.42\,\text{A}$.

The effectiveness of the proposed chattering suppression algorithm is demonstrated in Fig. 18.27, which represents the input current, output voltage and control command of a 4-phase DC/DC converter, respectively. The reference output voltage is 5 V. As it can be seen, the current chattering amplitude is 0.095, which is five times less than the current chattering amplitude of the 1-phase DC/DC converter.

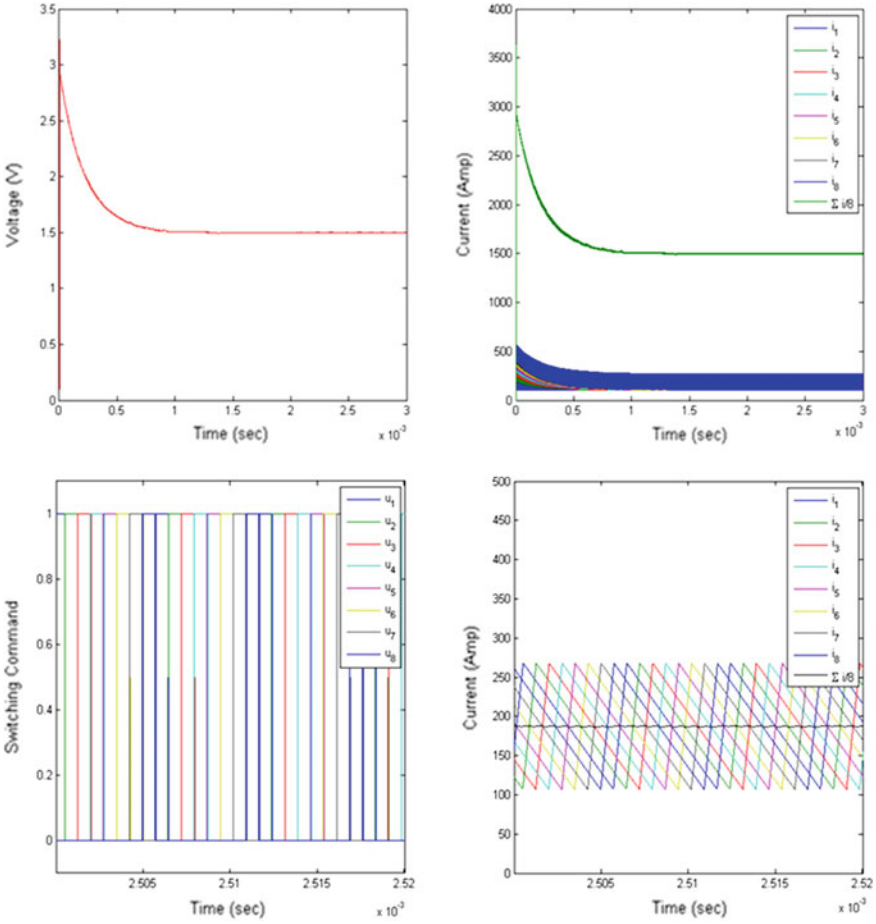

Fig. 18.22 Simulation results for the eight-phase DC/DC converter, $V_{ref} = 1.5\,\mathrm{V}$

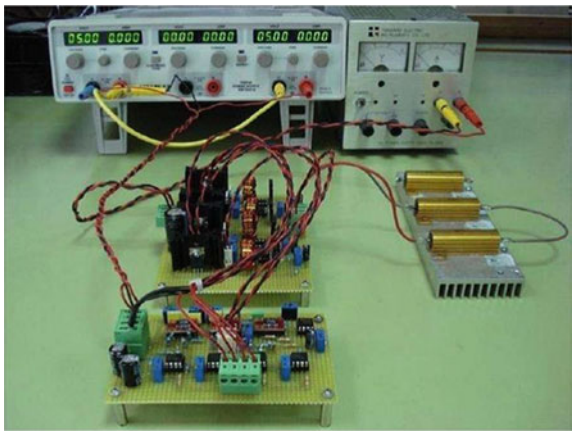

Fig. 18.23 Experimental Setup of a 4-phase DC/DC buck converter [2]

Table 18.6 Parameters of the experimental setup (4-phase DC/DC buck converter) [2]

L (H)	C (F)	R_L (Ω)	E (V)	*Switching Frequency*
22 μ	10 μ	2	10	100 KHz

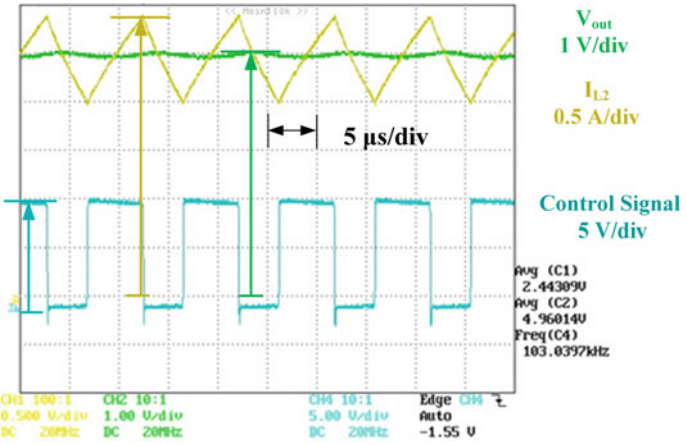

Fig. 18.24 Input current, output voltage and command control of a 1-phase DC/DC converter, $v_{dc\_ref} = 5\,\mathrm{V}$

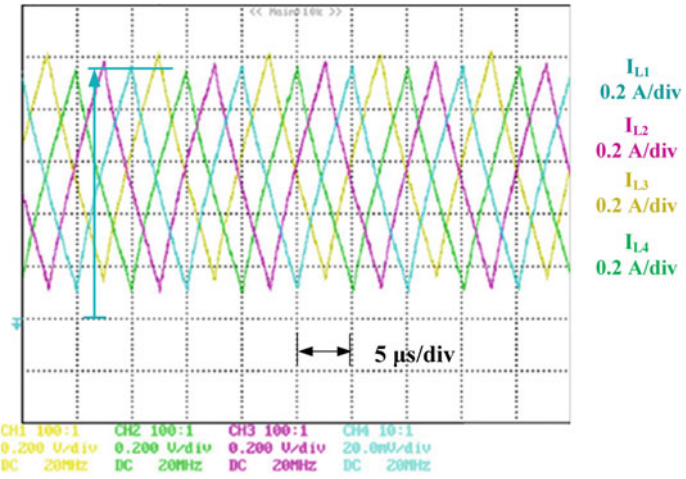

Fig. 18.25 Input phase currents a 4-phase DC/DC converter

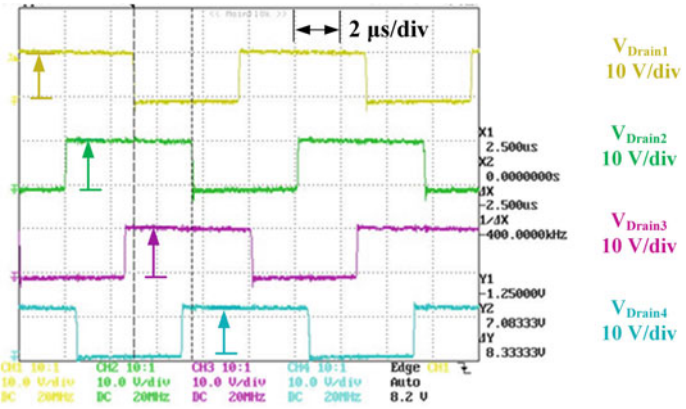

Fig. 18.26 MOSFET drain voltages of a 4-phases DC/DC converter

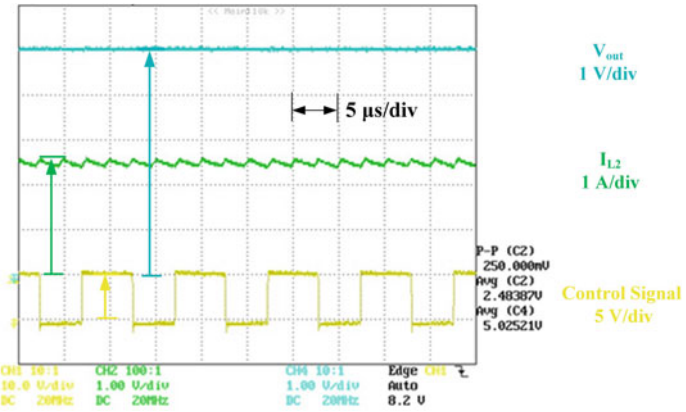

Fig. 18.27 Input current, output voltage and command control of a 4-phase DC/DC converter, $v_{dc\_ref} = 5\,\mathrm{V}$

Figure 18.28, shows the input current, output voltage and control command of a 4-phase DC/DC converted, where the reference output voltage is 4.59 V. It can be noticed that the algorithm almost cancelled the chattering completely. The average value of the output current is 2.28 A, with a chattering width of 0.033, which is about 14 times less than the current chattering amplitude of the 1-phase DC/DC converter. This is due to the fact that the four duty cycles are equal to 0.5, and the corresponding Fourier harmonic coefficients cancel each other.

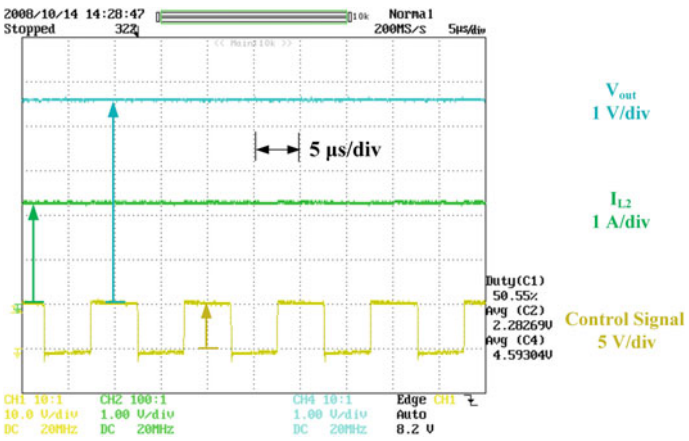

Fig. 18.28 Input current, output voltage and command control of a 4-phase DC/DC converter, $v_{dc\_ref} = 4.59\,\mathrm{V}$

18.3 Sliding Mode Control of AC/DC Power Converters

Recently, a variety of power electronic devices, including three-phase AC/DC power converters, has been widely used in energy conversion systems [28]. One of their disadvantages is that they cause inherent problems of reactive power generation and higher harmonic content in the input current. These practical problems have become more serious as the AC/DC converter capacity becomes much larger [8, 30, 44].

The ideal AC/DC converter has a constant dc output voltage (or current) and a pure sinusoidal input current at unity power factor from the ac line. Conventional thyristor phase-controlled converters have an inherent drawback which is that the power factor decreases as the firing angle increases and that harmonics of the line current are relatively high [21, 46]. In recent years, there has been a tendency to operate AC/DC converters with PWM switching patterns to improve the input and output performance of the converter. PWM AC/DC converters offer distinct advantages over the conventional rectifiers [15, 47]. These advantages include unity power factor, capability of bidirectional power flow, low harmonic components in input current and low ripple in output voltage. All of these features simplify filtering problems on both ac and dc sides of the converter [8, 39, 47].

The objective of this section is to develop a feedback control algorithm for AC/DC power converters such that the output voltage is maintained at the desired level with zero steady state error, input currents are free of higher harmonics and the reactive power is equal to zero. This mission will be accomplished using the framework of SMC methodology implying that the order of the motion is reduced with state trajectories in the pre-selected manifold with the system state space. Furthermore, the control system is designed in two reference frames: the abc natural reference frame, and the dq synchronous reference frame.

18.3.1 Circuit Model and Design Methodology

The circuit model and analysis of the three-phase PWM AC/DC voltage source converter in the natural *abc* and the rotating *dq* reference frames is presented next. First, consider the three-phase PWM AC/DC voltage source converter shown in Fig. 18.29, where e_a, e_b, e_c are the balanced three-phase AC voltages representing the infinite bus, $R_g$and L_g represent the grid-side resistance and inductance, respectively, C_{dc} is the dc-link capacitance, i_a, i_b, i_c are the three-phase AC input currents, i_{dc} is dc-link current, v_{dc} is dc-link voltage and i_L is the load current.

Based on circuit analysis, the AC input current equations are given by:

$$L_g \frac{di_a}{dt} = e_a - R_g i_a - v_{an} \tag{18.89}$$

$$L_g \frac{di_b}{dt} = e_b - R_g i_a - v_{bn} \tag{18.90}$$

$$L_g \frac{di_c}{dt} = e_c - R_g i_c - v_{cn} \tag{18.91}$$

where v_{an}, v_{bn}, v_{cn} are the voltages from the AC side of the converter to the power neutral point n. The balanced three-phase AC voltages are expressed as:

$$e_a = E_0 \sin(\omega t) \tag{18.92}$$

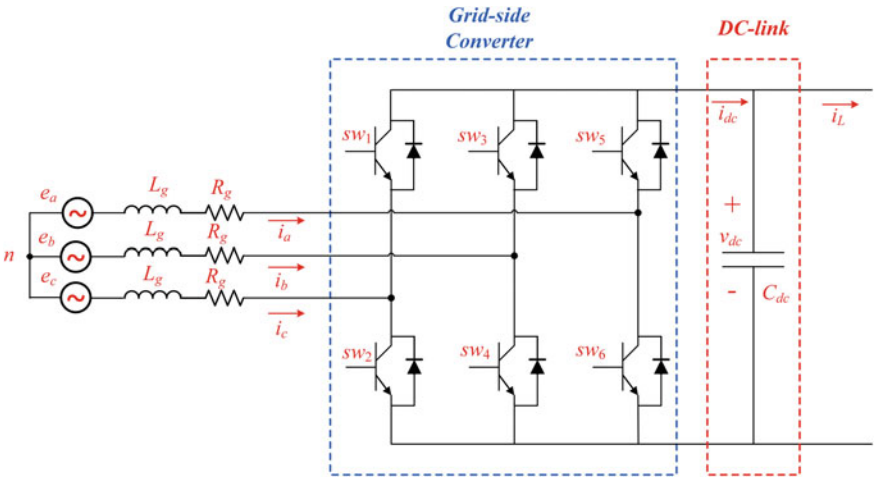

Fig. 18.29 Three-phase PWM AC/DC voltage source converter scheme

$$e_b = E_0 \sin\left(\omega t - \frac{2\pi}{3}\right) \tag{18.93}$$

$$e_c = E_0 \sin\left(\omega t + \frac{2\pi}{3}\right) \tag{18.94}$$

where E_0 is the amplitude of the phase voltage and ω is the ac power source angular frequency. If we assume that $i = \begin{bmatrix} i_a \\ i_b \\ i_c \end{bmatrix}$, $e = \begin{bmatrix} e_a \\ e_b \\ e_c \end{bmatrix}$, $v_s = \begin{bmatrix} v_{an} \\ v_{bn} \\ v_{cn} \end{bmatrix}$, then equations in (18.89)–(18.91) can be re-written in a compact form as:

$$L_g \frac{di}{dt} = e - R_g i - v_s \tag{18.95}$$

The switching function S of each switch can be defined as:

$$S_j = \begin{cases} 1 & S_j \quad is\ close \\ -1 & S_j \quad is\ open \end{cases} \quad j = a, b, c \tag{18.96}$$

The voltage vector v_s be expressed in terms of the switching functions $S = \begin{bmatrix} S_a \\ S_b \\ S_c \end{bmatrix}$ as:

$$v_s = \frac{1}{3} v_{dc} \begin{bmatrix} 2 & -1 & -1 \\ -1 & 2 & -1 \\ -1 & -1 & 2 \end{bmatrix} S \tag{18.97}$$

By substituting Eq. (18.97) into (18.95), the AC input current equations can be expressed as:

$$L_g \frac{di}{dt} = e - R_g i - \frac{1}{3} v_{dc} \begin{bmatrix} 2 & -1 & -1 \\ -1 & 2 & -1 \\ -1 & -1 & 2 \end{bmatrix} S \tag{18.98}$$

Finally, the output voltage equation can be given by:

$$C \frac{dv_{dc}}{dt} = -i_L + i^T S \tag{18.99}$$

The operating principle of the three phase PWM grid-side voltage source converter can also be analyzed by the classical rotating field theory with the well-known *Park and Clarke* transformations. The dynamic model of three-phase AC/DC voltage source converter in the *d-q* rotating reference frame can be described as [28]:

$$L_g \frac{di_d}{dt} = e_d - R_g i_d + \omega_g L_g i_q - v_d \tag{18.100}$$

$$L_g \frac{di_q}{dt} = e_q - R_g i_q - \omega_g L_g i_d - v_q \tag{18.101}$$

$$C \frac{dv_{dc}}{dt} = -i_L + \frac{1}{2}(i_d s_d + i_q s_q) \tag{18.102}$$

where, $v_d = v_{dc} s_d$ and $v_q = v_{dc} s_q$. s_d and s_q are the switching functions in the d-q synchronous reference frame. i_d, i_q, e_d and e_q are the input currents of the converter and grid voltages in the synchronous d-q reference frame, respectively. Note that $v_{dc} = v_{dc\_d}$ due to the field orientation.

The design methodology proposed in this chapter is different compared to the one usually used for AC/DC power converters. It is common to start with solving the main problem of maintaining the DC output voltage at the desired level and then minimizing high order harmonics and reactive power at the input. In this chapter, the inverse sequence of actions is offered. First, a tracking system is designed with sinusoidal current references proportional to the input AC voltages. This means that the reactive power is automatically equal to zero. If the tracking system is ideal, the input current will be free of higher harmonics. The second phase of the research work is the output voltage control. It will be shown that the output voltage will be constant and depends only on the amplitude of the reference input if designing the ideal tracking system is accomplished.

Furthermore, the proposed strategy does not utilize conventional SMC. As previously mentioned, the objective is to control three variables: two phase current and output voltage, using three dimensional control vectors. Generally, this can be done by enforcing sliding mode at the intersection of three sliding surfaces that depend on the mismatches between the reference and real values. However, the following analysis will show that matrix multiplying control is singular and conventional SMC methodology is not applicable.

18.3.2 Proposed Control Scheme in the abc Natural Reference Frame

(A) Sliding Mode Current Tracking Control

According to the proposed design procedure, phase currents should track sinusoidal reference inputs proportional to input ac voltages. The tracking problem is solved in the framework of sliding mode methodology. Substituting Eq. (18.100) into (18.99) results in:

$$L \frac{di_{abc}}{dt} = e_{abc} + v_{dc} \Gamma_0 S \tag{18.103}$$

where, matrix Γ_0 is given by:

$$\Gamma_0 = \begin{bmatrix} \frac{-2}{3} & \frac{1}{3} & \frac{1}{3} \\ \frac{1}{3} & \frac{-2}{3} & \frac{1}{3} \\ \frac{1}{3} & \frac{1}{3} & \frac{-2}{3} \end{bmatrix}, \quad det\Gamma_0 = 0 \tag{18.104}$$

Since the sum of the three-phase currents is equal to zero, three state variables should only be controlled: output voltage and two phase currents in a system with a three dimensional control vector S. But, unfortunately the conventional sliding mode method cannot be applied directly since matrix Γ_0 is singular. Because of that, we will start with designing a tracking system for two phase currents only. It means that sliding mode should be enforced on the intersection of two surfaces $\sigma_a = L\left(i_{aref} - i_a\right)$ and $\sigma_b = L\left(i_{bref} - i_b\right)$ or in vector form:

$$\sigma_{ab} = L\left(i_{abref} - i_{ab}\right) \tag{18.105}$$

Excluding the phase current $i_c = -i_a - i_b$ yields to:

$$L\frac{di_{ab}}{dt} = e_{ab} + u_c \Gamma S \tag{18.106}$$

$$C\frac{dv_{dc}}{dt} = -\frac{v_{dc}}{R} + (i_a, i_b, -i_a - i_b)S \tag{18.107}$$

where Γ is a 2×3 matrix given by:

$$\Gamma = \begin{bmatrix} \frac{-2}{3} & \frac{1}{3} & \frac{1}{3} \\ \frac{1}{3} & \frac{-2}{3} & \frac{1}{3} \end{bmatrix} \tag{18.108}$$

The ideal tracking system is based on Lyapunov function:

$$V = \frac{1}{2}\,\sigma_{ab}{}^T\ \sigma_{ab} \tag{18.109}$$

Discontinuous control should be selected such that time derivative of V is negative definite. The time derivative $\dot{V}$ on the system trajectory can be easily calculated as:

$$\dot{V} = \sigma_{ab}{}^T F\,(.) - \ u_c\,(\alpha, \beta, \gamma)\ S \tag{18.110}$$

where $F\,(.)$ is state function, which does not depend on control. α, β and γ are given by:

$$\begin{cases} \alpha = \left(\frac{-2}{3}\sigma_a + \frac{1}{3}\sigma_b\right) \\ \beta = \left(\frac{1}{3}\sigma_a + \frac{-2}{3}\sigma_b\right) \\ \gamma = \left(\frac{1}{3}\sigma_a + \frac{-2}{3}\sigma_b\right) \end{cases} \tag{18.111}$$

If v_{dc}/L is large enough, $F(.)$ can be suppressed with control S given by:

$$S = \begin{cases} S_a = sign\ (\alpha) \\ S_b = sign\ (\beta) \\ S_c = sign\ (\gamma) \end{cases} \tag{18.112}$$

where α, β and γ are selected such that $\dot{V} < 0$. This means that σ_{ab} tends to zero. Even more, σ_{ab} becomes zero after a finite time interval t_s [10]. As a result, sliding mode occurs with $i_{ab} = i_{abref}$. If a tracking system is designed with sinusoidal current references proportional to the input AC voltages as:

$$i_{ab} = K * e_{ab} \tag{18.113}$$

where K is constant. Then, the first problem of having zero reactive power and phase currents free of higher harmonics is solved.

(B) Sliding Mode Output Voltage Control

The main objective is to maintain the DC output voltage at the desired level. The first question to be answered is what is the output voltage after sliding mode occurs? Sliding mode equation can be derived using the so called "equilibrium control" procedure [39]. Step 1: time derivative of vector σ_{ab} on the state trajectory is made equal to zero. Step 2: the obtained algebraic equation should be solved with respect to control S and then substituted in the original system.

The equivalent control:

$$(\Gamma S)_{eq} = \left(L\frac{di_{abref}}{dt} - e_{ab}\right)\frac{1}{u_c} \tag{18.114}$$

is the solution of the following equation:

$$\frac{d\sigma_{ab}}{dt} = L\frac{di_{abref}}{dt} - e_{ab} - v_{dc}(\Gamma S)_{eq} = 0 \tag{18.115}$$

The three phase input currents can also be written as:

$$\left(i_a,\ i_b,\ -i_a - i_b\right) = -\left(i_a - i_c,\ i_b - i_c\right)\ \Gamma \tag{18.116}$$

After substituting Eqs. (18.114) and (18.115) into (18.107), the sliding mode equation can be obtained as:

$$C\left(\frac{dv_{dc}}{dt}\right)=\left(-\frac{v_{dc}}{R}\right)-\frac{L}{u_c}\left(i_a\frac{di_a}{dt}+i_b\frac{di_b}{dt}+ic\frac{di_c}{dt}\right)+\frac{1}{v_{dc}}\ (i_ae_a+i_bi_b+i_ce_c) \tag{18.117}$$

For the given balanced three phase input voltages given by Eqs. (18.88)–(18.91), and after sliding mode occurs ($i_{ab}=Ke_a$), it can be noticed that:

$$\begin{cases} i_a\frac{di_a}{dt}+i_b\frac{di_b}{dt}+i_c\frac{di_c}{dt}=0 \\ i_ae_a+i_be_b+i_ce_c=\frac{3}{2}K{E_0}^2=costant \end{cases} \tag{18.118}$$

After substituting Eq. (18.118) into (18.117), the sliding mode equation is given by:

$$C\frac{dv_{dc}}{dt}=-\frac{v_{dc}}{R_L}+\frac{3}{2}K{E_0}^2\frac{1}{u_c} \tag{18.119}$$

The last equation has only one asymptotically stable equilibrium point that can be described by:

$$v_{dcss}=\sqrt{\frac{3}{2}K{E_0}^2R_L} \tag{18.120}$$

In order to prove the stability of the equilibrium point, represent the right hand side of Eq. (18.119) in the form:

$$\begin{cases} f\ (v_{dc})=-\frac{v_{dc}}{R_L}+\frac{3}{2}K{E_0}^2\frac{1}{u_c} \\ f\ (v_{dc})=-g\ (v_{dc})\ (v_{dc}-v_{dcss})\ ,\ g\ (v_{dc})>0 \\ \Delta v_{dc}=(v_{dc}-v_{dcss}) \end{cases} \tag{18.121}$$

The derivative of $f\ (v_{dc})$ is negative and is given by:

$$f'\ (v_{dc})=-\frac{1}{R_L}-\frac{3}{2}K{E_0}^2\frac{1}{v_{dc}^2}<0 \tag{18.122}$$

Therefore, $g\ (u_c)>0$ and $C\frac{d\Delta u_c}{dt}=-g\Delta u_c$, $\Delta u_c\to 0$. This proves that the equilibrium point of (18.119) is asymptotically stable. It can be seen that the output voltage tends to a constant value which depends on the value of constant K in the reference current input equation. If R_L is known, K can be easily assigned. Otherwise, K should be varied such that the equilibrium point is equal to desired value u_{cref}. As in any boost converter, the output voltage should be greater than some minimum value. Correspondingly, $K>K_{min}$ and $K_{min}>0$. Selected K as an integral function of the mismatch as:

$$\dot{K} = \alpha \left(u_{cref} - u_c\right) + M\, sg\left(K_{min} - K\right),\ \alpha > 0,\ M > \alpha \left|v_{dc\_ref} - v_{dc}\right| \tag{18.123}$$

where α is constant. The last term of (18.123) is added to prevent K from being less than K_{min}. The only steady state of the system is $u_c = u_{cref}$, and the value of K is given by:

$$K = \frac{2}{3}\frac{v_{dc\_ref}^2}{{E_0}^2 R_L} \tag{18.124}$$

If $v_{dc\_ref} > 0$, $K(0) > 0$, and $v_{dc}(0) > 0$, then, according to (18.120) and (18.123), $K(t) > 0$ and $v_{dc}(t) > 0$ for any $t > 0$. Substituting $u_c = u_{cref} + x > 0$ in Eq. (18.120) results in:

$$\frac{dx}{dt} = -Av_{dc_{ref}} - Ax + \frac{BK}{v_{dc_{ref}} + x} \tag{18.125}$$

Differentiating Eq. (18.125) results in:

$$\ddot{x} = -(t)\dot{x} - f(x),\ (t) > 0,\ x\, f(x) > 0 \tag{18.126}$$

Select the Lyapunov function:

$$V = \frac{\dot{x}^2}{2} + \int_0^x f(\gamma)d\gamma > 0 \tag{18.127}$$

The time derivative $\dot{V}$ on the system trajectory can be easily calculated as:

$$\dot{V} = -(t)\dot{x}^2 \tag{18.128}$$

Since $\dot{x}(t) \equiv 0$, this means that $x(t) \equiv 0$ and the equilibrium point is globally asymptotically stable.

18.3.3 Proposed Control Scheme in the dq Synchronous Reference Frame

(A) Sliding Mode Current Tracking Control

Similar to the control design for electric motors, the current control of a *Boost*-type AC/DC power converter can be designed either in phase coordinates or in the dq coordinate frame. Since the control criteria (as listed in the performance characteristics) are normally given in the dq coordinate frame, it is more convenient to design the current control in the dq coordinate frame than in phase coordinates. Represent the current equations in (18.100) and (18.101) in a vector form as:

$$\dot{I}_{dq} = f_{dq}(I_{dq}, e_{dq}, \omega_g) - bs_{dq} \tag{18.129}$$

where,

$$\begin{cases} I_{dq} = \begin{bmatrix} i_d \\ i_q \end{bmatrix} \\ s_{dq} = \begin{bmatrix} s_d \\ s_q \end{bmatrix} \\ f_{dq}\left(I_{dq}, e_{dq}, \omega_g\right) = \begin{bmatrix} \frac{R_g}{L_g} i_d + \frac{e_d}{L_g} + \omega_g i_q \\ -\frac{R_g}{L_g} i_q + \frac{e_q}{L_g} - \omega_g i_d \end{bmatrix} \\ b = \frac{v_{dc}}{2L} \end{cases} \tag{18.130}$$

The switching functions for the current control are designed as:

$$\sigma_d = i_d^* - i_d \tag{18.131}$$

$$\sigma_q = i_q^* - i_q \tag{18.132}$$

where i_d^* and i_q^* are the desired values of the currents in the (d, q) coordinate frame. The next task is to find the condition under which sliding mode can be enforced. It can be noticed that no control gain can be adjusted for the control design of AC/DC converters. The solution is to find a domain in the system space from which any state trajectory converges to the sliding manifold defined by $\sigma_d = 0$, $\sigma_q = 0$. Defining $\sigma_{dq} = [\sigma_d, \sigma_q]^T$ and taking the time derivative of σ_{dq} results in:

$$\dot{\sigma}_{dq} = \dot{I}_{dq}^* - f_{dq}\left(I_{dq}, e_{dq}, \omega_g\right) + b\, s_{dq} = F_{dq} + DS \tag{18.133}$$

where $I_{dq}^* = [i_d^*, i_q^*]^T$, $F_{dq} = \dot{I}_{dq}^* - f_{dq}\left(I_{dq}, e_{dq}, \omega_g\right)$, $D = bA_{d,q}^{\alpha,\beta} A_{\alpha,\beta}^{a,b,c}$, $A_{d,q}^{\alpha,\beta} A_{\alpha,\beta}^{a,b,c}$ are the Park and Clarke transformation matrices, respectively, S is the vector of transformed switching functions defined in (18.8).

Design the matrix of switching functions S as:

$$S = -sign(S^*) \tag{18.134}$$

where $S^* = [S_a^*, S_b^*, S_c^*]^T$ is a vector of transformed switching functions and $sign\,(S^*) = [sign(S_a^*), sign(S_b^*), sign(S_c^*)]^T$. The transformed vector S^* should be designed such that, s_{fd} and s_{fq} disappear in finite time. Vector S^* is selected as:

$$S^* = \frac{3}{2b^2} D^T \sigma_{dq} \tag{18.135}$$

Design a *Lyapunov* function candidate as:

$$V = \sigma_{dq}^T \sigma_{dq} \tag{18.136}$$

The time derivative of the *Lyapunov* function on the system trajectory can be easily calculated as:

$$\dot{V} = (S^*)^T F^* + (S^*)^T D^T D S \tag{18.137}$$

where $F^* = [\, F_a^* \;\; F_b^* \;\; F_c^* \,]^T = D^T F_{dq}$. Substituting control equation (18.134) into (18.137) results in:

$$\dot{V} = (S^*)^T F^* - \left(S^*\right)^T D^T D \; sign(S^*) \tag{18.138}$$

where $D^T D$ is a singular matrix that can be calculated as:

$$D^T D = b^2 \frac{4}{9} \begin{bmatrix} 1 & -\frac{1}{2} & -\frac{1}{2} \\ -\frac{1}{2} & 1 & -\frac{1}{2} \\ -\frac{1}{2} & -\frac{1}{2} & 1 \end{bmatrix} \tag{18.139}$$

Equation (18.138) can be expanded as:

$$\dot{V} = \left(S_a^* F_a^* + S_b^* F_b^* + S_c^* F_c^*\right) - \left(\frac{2}{3}\right)^2 b^2 \left(2\left|S_l^*\right| + \left|S_m^*\right| + \left|S_n^*\right|\right) \tag{18.140}$$

where $l \neq m \neq n \; and \; l, m, n \; \in \{a, b, c\}$. Equation (18.140) can be further represented as:

$$\dot{V} = \left(S_a^* F_a^* + S_b^* F_b^* + S_c^* F_c^*\right) - \left(\frac{2}{3}\right)^2 b^2 \left(\left|S_l^*\right| + \left|S_m^*\right| + \left|S_n^*\right|\right) - \left(\frac{2}{3}\right)^2 b^2 \left|S_l^*\right| \tag{18.141}$$

This means that the sufficient condition for $\dot{V} < 0$ can be given by:

$$\left(\frac{2}{3}\right)^2 b^2 > \max(F_a^*, F_b^*, F_c^*) \tag{18.142}$$

Equation (18.142) defines a subspace in the system space in which the state trajectories converges to the sliding manifold defined by $\sigma_{dq} = 0$ in finite time. This is to show that the attraction domain in the sliding manifold is bounded in the state space. It is also important to notice that parameter $b = \frac{v_{dc}}{2L}$ should be high enough at the initial time instant. The output voltage is not zero at the initial time instant since $v_{dc\_d} = v_{dc}$. In critical applications, this can be achieved by starting the converter operation with an open-loop control. The last step of the current control design is that the resulting controls S_a, S_b and S_c should be mapped into the switching patterns

that can be applied to the power converter. This can be done using the following system of equations:

$$\begin{cases} s_{w1} = \frac{1}{2}\left(1 + S_a\right), s_{w4} = 1 - s_{w1} \\ s_{w2} = \frac{1}{2}\left(1 + S_b\right), s_{w5} = 1 - s_{w2} \\ s_{w3} = \frac{1}{2}\left(1 + S_c\right), s_{w6} = 1 - s_{w3} \end{cases} \tag{18.143}$$

(B) Sliding Mode Output Voltage Control

It is necessary to determine the reference currents feeding to the current controller, i_d^* and i_q^*, in order to ensure asymptotic stability of the output voltage regulation. Neglecting the voltage drop over the phase resistance R_g, Eqs. (18.100)–(18.102) can be simplified to:

$$L_g \frac{di_d}{dt} = e_d + \omega_g L_g i_q - v_d \tag{18.144}$$

$$L_g \frac{di_q}{dt} = e_q - \omega_g L_g i_d - v_q \tag{18.145}$$

$$C\frac{dv_{dc}}{dt} = -i_L + \frac{1}{2}(i_d s_d + i_q s_q) \tag{18.146}$$

In general, the value of the inductance satisfies $L \ll 1$, while the right-hand sides of equations in (18.144)–(18.146) have the values of the same order. Therefore, $di_d/dt, di_q/dt \gg du_{cd}/dt$ indicating that the dynamics of i_d and i_q are much faster than those of v_{dc}. In case that the fast dynamics are stable, the output voltage control can be simplified considerably. Based on the *Singular Perturbation Theory* [19, 20], the left-hand sides of Eqs. (18.144)–(18.146) can be formally equal to zero, and the algebraic equations for s_d and s_q can be solved. Therefore, the following equation system is valid for control design of the slow-manifold:

$$s_d = \frac{2\left(e_d + \omega_g L i_q^*\right)}{v_{dc}} \tag{18.147}$$

$$s_q = \frac{2\left(e_q + \omega_g L i_d^*\right)}{v_{dc}} \tag{18.148}$$

$$\frac{dv_{dc}}{dt} = -\frac{i_L}{C} + \frac{i_d^* s_d + i_q^* s_q}{2C} \tag{18.149}$$

where i_d^* and i_q^* are the reference values of i_d and i_q, respectively. The real currents are replaced with their reference values in Eqs. (18.147) and (18.149), since we assume that the inner current control loop is in sliding mode with $\sigma_d = i_d^* - i_d, \sigma_q = i_q^* - i_q$.

As mentioned in the introduction, the objective is to control the three-phase AC/DC power converter such that the output voltage is maintained at the desired level with zero steady state error, input currents are free of higher harmonics and the reactive power is equal to zero. The demand of sinusoidal input currents has been fulfilled automatically by involving the (*d*,*q*) transformation. The following characteristics will cover the remaining major requirements of a well-controlled three-phase AC/DC power converter:

1. The output voltage should converge to its reference value u_c^*.
2. The input current phase-angle, $\rho^* = \arctan(i_q^*/i_d^*)$, should trace its reference value.
3. The power-balance condition should be satisfied, i.e. $e_d i_d^* + e_q i_q^* = u_c^* i_l = v_{dc}^* i_L$.

The reference currents i_d^* and i_q^* should be calculated satisfying these requirements. Substitution of (18.147) and (18.148) into (18.149) yields:

$$\frac{dv_{dc}}{dt} = -\frac{i_L}{C} + \frac{i_d^* s_d + i_q^* s_q}{C v_{dc}} \tag{18.150}$$

Taking into account the power-balance condition, the above equation can be simplified to:

$$\frac{dv_{dc}}{dt} = -\frac{i_L}{C} + \frac{v_{dc}^* i_L}{C v_{dc}} \tag{18.151}$$

For a system with a pure load resistance R_L, $i_L = v_{dc}/R_L$. As a result, linear dynamics for output voltage u_{cd} can be calculated as:

$$\frac{dv_{dc}}{dt} = \frac{v_{dc}^* - v_{dc}}{C R_L} \tag{18.152}$$

Define the voltage regulation error as $\bar{v}_{dc} = v_{dc}^* - v_{dc}$ with a constant desired voltage $\dot{v}_{dc}^* = 0$ such that:

$$\bar{v}_{dc} + R_L C \dot{\bar{v}}_{dc} = 0 \tag{18.153}$$

Equation (18.153) shows that the voltage error tends to zero asymptotically with the time-constant $R_L C$. It also means that the output voltage converges to its reference value automatically if the power-balance condition is fulfilled. Finally, i_d^* and i_q^* can be calculated as:

$$i_d^* = \frac{v_{dc}^* i_L}{e_d + e_d tan\rho^*} \tag{18.154}$$

$$i_q^* = \frac{v_{dc}^* i_L \tan\rho^*}{e_d + e_d \tan\rho^*} \tag{18.155}$$

where ρ^* is the input reference current phase angle. It is usually determined by the control designer.

18.3.4 Simulation Results

In order to evaluate the proposed sliding mode control strategies for AC/DC power converters, several computer simulations have been conducted using MATLAB/Simulink software. Parameters of the simulated three-phase AC/DC converter are listed in Table 18.7. All of the reported results were obtained under the assumption that ideal sliding modes are enforced in the systems. Figure 18.30 shows the DC output voltage using the proposed SMC algorithm. As it can be seen, the output voltage is maintained at the desired level with zero steady state error. $v_{dc\_ref} = 250\,\text{V}$ in this case,

Results of the current tracking control system are shown in Fig. 18.31. After the transient stage, phase currents track references very well. This proves that the proposed sliding mode control strategy ensures that the input currents are free of higher order harmonics.

Figure 18.32 shows the source voltage and current. It illustrates the ability of the proposed control algorithm to reduce the reactive power to zero and maintain a unity power factor.

Figure 18.33 illustrates the ability of the input current and output voltage control systems under the proposed strategy to quickly follow a sudden change in the dc link voltage reference ($v_{dc\_ref1} = 300\,\text{V}$, $v_{dc\_ref2} = 250\,\text{V}$). In this case, K should be

Table 18.7 Simulation parameters of the three-phase AC/DC converter

Parameter	L (mH)	C (μf)	f (Hz)	R_L (Ω)	E_0 (V)
Value	7.5	820	60	100	120

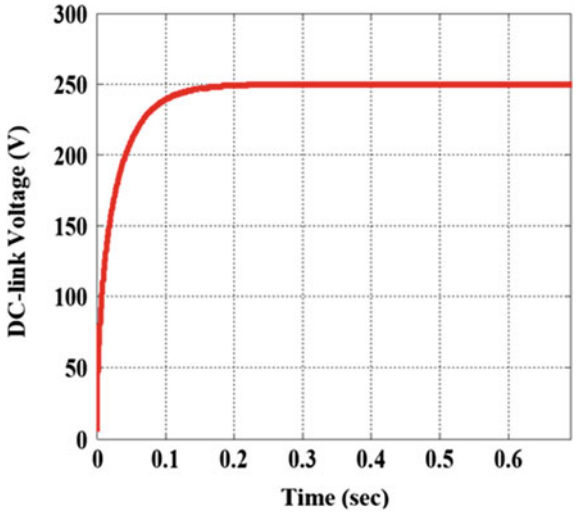

Fig. 18.30 DC-link output voltage of the AC/DC power converter

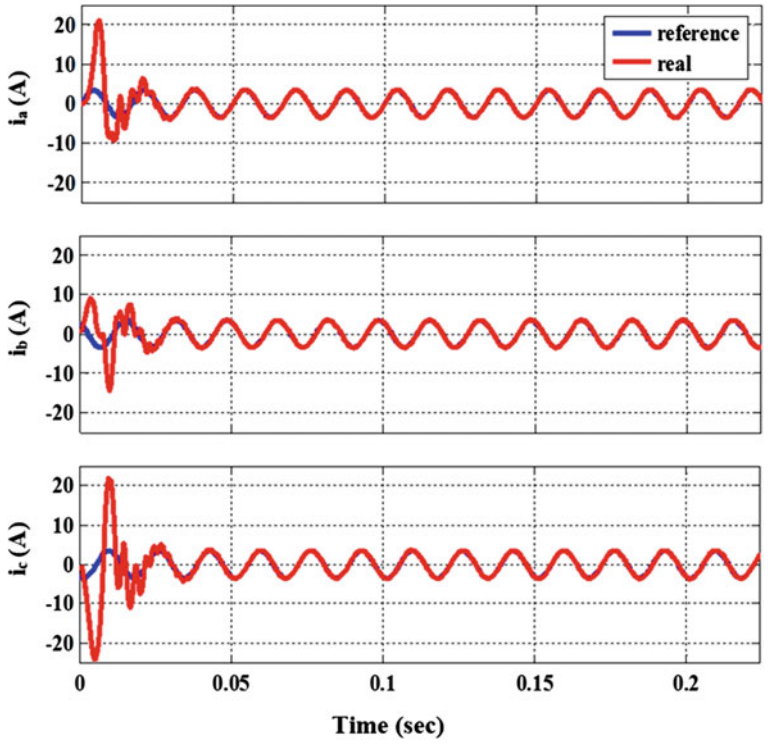

Fig. 18.31 Three-phase current tracking using the proposed SMC strategy

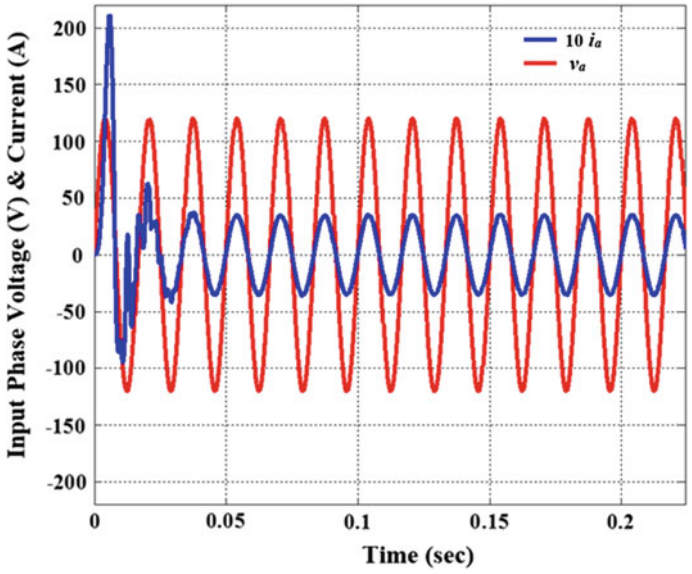

Fig. 18.32 Input phase voltage and phase current

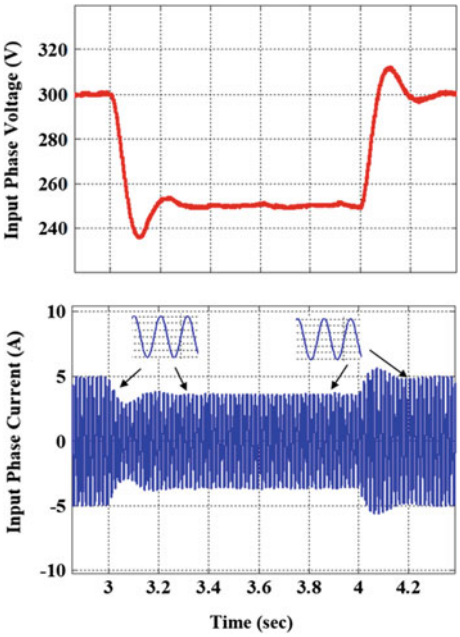

Fig. 18.33 System response to a sudden change of the dc link voltage and input current

varied such that the equilibrium point is equal to desired value u_{cref}. For this purpose, K is selected as an integral function of the mismatch $v_{dc\_ref} - v_{dc}$.

18.4 Sliding Mode Control of DC/AC Power Electronic Inverters

PWM originally refers to an approach used to realize or amplify a continuous function by using on/off implementation. In power electronics industry, the term PWM also refers to the control of semiconductor switches in converter circuits. With the development of new control algorithms for power converters, several PWM techniques have been proposed and implemented in the control system of DC/AC inverters, like harmonic elimination PWM [5, 6] space vector PWM [17, 18, 41], sine-triangle PWM [28], hybrid PWM [3], hysteresis band control, etc.

PWM control approaches can be classified into two main categories: open-loop control using a pre-calculated switching pattern, such as harmonic elimination PWM, and close-loop control whose switching actions depend on feedback information, such as hysteresis band PWM approach. Some of them can be used in both open-loop and close-loop schemes, such as space vector PWM [41]. Comparative studies of different PWM techniques can be found in [31, 37], and other literature.

Performance of power electronic inverters is evaluated in different aspects, for instance harmonic loss factor, reference tracking ability and robustness against variation of circuit parameters and disturbances. Therefore, Sliding mode control (SMC) is very natural to be used in the control of power inverters [1, 38–40], since the switching between two discrete values can be used directly as gating signals to the semiconductor switching devices in power converter circuits. SMC has excellent reference tracking ability and robust against parameter variations of the inverter.

This section presents a new PWM approach for power electronic inverters called Sliding Mode PWM (SMPWM). It is a close-loop control method based on the sliding mode concept. The control objective is to track proper reference inputs using a three-phase full-bridge inverter. It considers the fact that three arbitrary phase current references cannot be tracked for three-phase three-wire systems.

18.4.1 Circuit Model and Design Methodology

Consider the system in Fig. 18.34. The three-phase full-bridge inverter under control is to provide desired currents to the load, taking into account that they can be dependent.

Based on circuit analysis, the system equations are:

$$\begin{cases} L\frac{di_a}{dt} + Ri_a + E_a = s_a\, U_{dc} - v_n \\ L\frac{di_b}{dt} + Ri_b + E_b = s_b U_{dc} - v_n \\ L\frac{di_c}{dt} + Ri_c + E_c = s_c\, U_{dc} - v_n \end{cases} \tag{18.156}$$

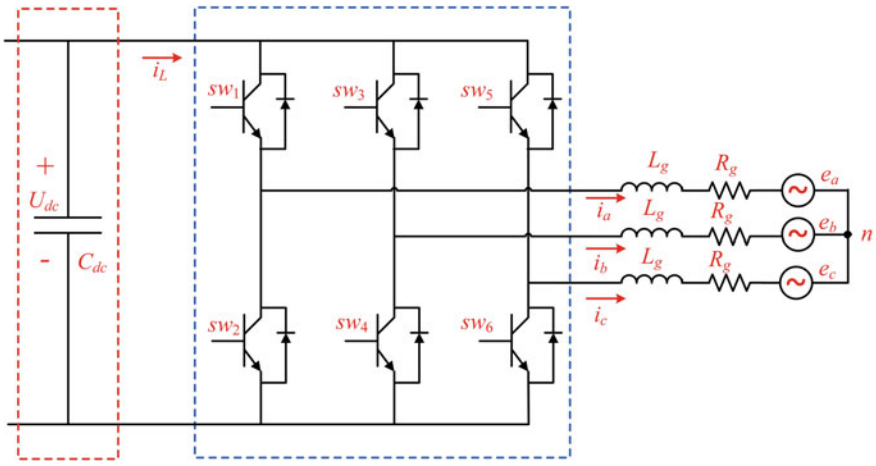

Fig. 18.34 Three-phase PWM DC/AC inverter scheme

where v_n is the voltage at neutral point. $E_a,\ E_b,\ E_c$ are balanced three phase voltage sources which represent three back EMF in ac motors. $s_a,\ s_b,\ s_c \in \{\pm 1\}$ represent the on/off control signals for six switching devices of the three-phase full-bridge converter. If a switching device is conducting, value "1" is assigned to it, otherwise "−1" is assigned. Since sum of the currents is equal to zero, v_n of the three-phase system can be found as:

$$v_n = \frac{U_{dc}}{3}(s_a + s_b + s_c) \tag{18.157}$$

It looks natural that v_n is discontinuous, but its average value changes continuously.

18.4.2 Sliding Mode Pulse Width Modulation (SMPWM)

The objective of the inverter's control system is to track proper selected voltage or current references. Some existing PWM techniques use three-phase current errors as inputs to its controller, for instance hysteresis band PWM. It controls the three phases independently based on corresponding current error. However, as it was mentioned, the three currents cannot be independent.

Denote

$$\begin{cases} J_a = -\left(\frac{R}{L}\right) i_a - \frac{E_a}{L} \\ J_b = -\left(\frac{R}{L}\right) i_b - \frac{E_b}{L} \\ J_c = -\left(\frac{R}{L}\right) i_c - \frac{E_c}{L} \end{cases} \tag{18.158}$$

Substituting (18.157) into (18.156) results in:

$$\frac{di}{dt} = J + \frac{U_{dc}}{3L} DS \tag{18.159}$$

where,

$$i = \begin{bmatrix} i_a \\ i_b \\ i_c \end{bmatrix},\ D = \begin{bmatrix} 2 & -1 & -1 \\ -1 & 2 & -1 \\ -1 & -1 & 2 \end{bmatrix},\ S = \begin{bmatrix} s_a \\ s_b \\ s_c \end{bmatrix},\ J = \begin{bmatrix} J_a \\ J_b \\ J_c \end{bmatrix}$$

Notice that matrix D is singular, therefore among i_a, i_b, i_c, only two phase currents can be controlled independently. If the sum of reference currents $\sum i_z^* \neq 0$, where $z = a, b, c$, then problem can not be solved. If $\sum i_z^* = 0$, only two of the reference inputs can be given independently, then we have one superfluous degree of freedom since the dimension of control equals to three. As result, although three currents are equal to the desired values, the motion of system is not unique. For example the voltage v_n in (18.157) can be equal to different values. In future, we assume that reference inputs and are given and discuss how to utilize the additional degree of freedom.

It should be noted from (18.156) that, since the equation for each phase current depends on all three discontinuous functions s_a, s_b, s_c, the frequency analysis cannot be performed independently. Thus, although hysteresis band PWM works in practical implementation, its analysis needs to be carefully checked. Control algorithm should be developed to control three-phase currents while only two of them can be controlled independently. The extra one degree of freedom can be used to control one more variable.

The proposed control algorithm is based on complementing the original system by the first order equation:

$$\dot{s}_3 = v_n^* - v_n \tag{18.160}$$

where v_n is defined in Eq. (18.157).

The sliding surfaces $s = [s_a, s_b, s_3]^T$ can be defined as:

$$\begin{cases} s_a = i_a^* - i_a \\ s_b = i_b^* - i_b \\ s_3 = \int (v_n^* - v_n)\, d\tau \end{cases} \tag{18.161}$$

where i_a^*, i_b^*, v_n^* are reference signals. The derivative of vector s can be easily derived as:

$$\begin{cases} \dot{s}_a = i_a^* - J_a - \frac{2}{3}\frac{U_{dc}}{L} s_a + \frac{1}{3}\frac{U_{dc}}{L} s_b + \frac{1}{3}\frac{U_{dc}}{L} s_c \\ \dot{s}_b = i_b^* - J_b - \frac{2}{3}\frac{U_{dc}}{L} s_b + \frac{1}{3}\frac{U_{dc}}{L} s_a + \frac{1}{3}\frac{U_{dc}}{L} s_c \\ \dot{s}_3 = v_n^* - (U_{dc}/3)\,(s_a + s_b + s_c) \end{cases} \tag{18.162}$$

Three-dimensional discontinuous control J can be designed such that sliding mode is enforced on $s = 0$. When sliding mode occurs on $s = 0$, all three components of are equal to zero and the tracking problem is solved. Since motion equation in sliding mode depends on parameter v_n^*, it can be selected in correspondence with some performance criterion. Different control methods can be used to enforce sliding mode.

Having proposed sliding surface s, the proposed control algorithm should be designed such that vector s is reduced to zero after finite time. Select the Lyapunov function:

$$V = \frac{1}{2} s^T s \tag{18.163}$$

Its time derivative is given by:

$$\dot{V} = F(.) - \frac{U_{dc}}{3L}[\alpha s_a + \beta s_b + \gamma s_c] \tag{18.164}$$

where,

$$\begin{cases} F(.) = s_a\left(i_a^* - J_a\right) + s_b\left(i_b^* - J_b\right) + s_3 v_n^* \\ \alpha = (2s_a - s_b + s_3 L) \\ \beta = (2s_b - s_a + s_3 L) \\ \gamma = (-s_a - s_b + s_3 L) \end{cases} \tag{18.165}$$

If u_c/L is large enough, $F(.)$ can be suppressed with control S given by:

$$S = \begin{cases} s_a = sign\ (\alpha) \\ s_b = sign\ (\beta) \\ s_c = sign\ (\gamma) \end{cases} \tag{18.166}$$

The proposed SMPWM control design for AC/DC inverters has the following advantages:

1. SMPWM with Lyapunov approach takes into account all sliding surfaces directly for each phase's control.
2. SMPWM does not require the dc voltage source to have constant value.
3. SMPWM can tolerate significant amount of disturbances or fluctuations from voltage source. This is an attractive advantage of SMPWM.

18.4.3 SMPWM Using Sliding Surface Decoupling Approach

Although the SMPWM method proposed in Sect. 4.2 is simple, it does not provide the capability to analyze the motion in the vicinity of the sliding manifold, since the three equations in (18.162) are interconnected. Therefore, this section presents another SMPWM technique that takes into account all sliding surfaces indirectly for each phase's switching control.

Equation (18.162) can be written in matrix form

$$\dot{s} = f_2 + \frac{U_{dc}}{3L} BJ \tag{18.167}$$

where the vector $f_2 = \left[\frac{di_a^*}{dt} - K_a, \frac{di_b^*}{dt} - K_b, v_n^*\right]$ includes terms without control variables, and $B = \begin{bmatrix} 2 & -1 & -1 \\ -1 & 2 & -1 \\ L & L & L \end{bmatrix}$. Since B is a non-singular matrix, it can be transformed into a diagonal matrix, and control variables can be decoupled for each sliding surface. Introduce new switching manifold $\bar{s} = B^{-1}s = 0$. In this case,

$$B^{-1} = \frac{1}{9L}\begin{bmatrix} 3L & 0 & 3 \\ 0 & 3L & 3 \\ -3L & -3L & 3 \end{bmatrix} \tag{18.168}$$

$$\bar{s} = \frac{1}{9L}\begin{bmatrix} 3Ls_a + 3s_3 \\ 3Ls_b + 3s_3 \\ -3Ls_a - 3Ls_b + 3s_3 \end{bmatrix} = \begin{bmatrix} \bar{s}_1 \\ \bar{s}_2 \\ \bar{s}_3 \end{bmatrix} \tag{18.169}$$

Differentiation of (18.169) gives $\dot{\bar{s}}_1 = B^{-1}\dot{s}$ and $\dot{s}$ can be as:

$$\dot{\bar{s}} = B^{-1}\dot{s} = f_3 - \frac{U_{dc}}{3L}\begin{bmatrix} s_a \\ s_b \\ s_c \end{bmatrix} \tag{18.170}$$

where $f_3 = [f_{31}, f_{32}, f_{33}]^T$ is a 3 * 1 vector whose elements have bounded values as:

$$\begin{cases} f_{31} = \frac{1}{3L}(L\frac{di_a^*}{dt} - LK_a + v_n^*) \\ f_{32} = \frac{1}{3L}(L\frac{di_b^*}{dt} - LK_b + v_n^*) \\ f_{33} = \frac{1}{3L}(-L\frac{di_a^*}{dt} + LK_a - \frac{di_b^*}{dt} + LK_b + v_n^*) \end{cases} \tag{18.171}$$

f_3 does not include control variables, s_a, s_b and s_c. Equation (18.170) shows that the overall motion can be decoupled into three individual ones (with respect to control). Select the control logic for inverter switches as follows:

$$\begin{cases} s_a = sign\ (\bar{s}_1) \\ s_b = sign\ (\bar{s}_2) \\ s_c = sign\ (\bar{s}_3) \end{cases} \tag{18.172}$$

If $\frac{U_{dc}}{3L} > \sup \|f_3\|$, the sliding mode existence conditions $\bar{s}_1\dot{\bar{s}}_1 < 0, \bar{s}_2\dot{\bar{s}}_2 < 0, \bar{s}_3\dot{\bar{s}}_3 < 0$ hold. Sliding manifold is reached after finite time. Reference input v_n^* can be selected depending on some operation criteria: control of switching frequency, minimization of this frequency with given accuracy, and so on.

18.4.4 Sliding Mode Control of Neutral Point Voltage (v_n)

This section explains the physical meaning of the proposed control methodology. As it follows from (18.162), the time derivative of s_3 depends on varying at high frequency in sliding mode. It means high frequency will be rejected on sliding surface and will depend on average value of v_n.

Section 4.3 shows that SMPWM can track reference currents and control the average value of v_n at the same time. As a result, proper v_n^* can be found to minimize some performance criterion. As an example, the switching frequency is to be minimized in order to reduce switching losses with a given accuracy. Ideally, sliding mode is a mathematical abstraction where the sliding motion trajectories are strictly on discontinuous surfaces. However, sliding mode in a real life system occurs not strictly on its discontinuous surfaces. Instead, it appears within some boundary layer. Analysis of sliding motion in boundary layer can be found in [40]. Assume that switching devices have hysteresis loop Δ. Then Δ defines the accuracy of the system, as shown in Fig. 18.35. In our system, the switching frequency depends on state velocities. Moreover, the switching frequency is not a constant value. We consider the system using surface decoupling approach shown in Sect. 4.3. Then each phase can be handled independently. The switching frequency is determined by two time intervals with $\dot{s} > 0$ and $\dot{s} < 0$. Consider the switching behavior of the i-th motion in (18.170) where $i \in \{1, 2, 3\}$. For each motion in (18.170), the time duration of "switch on" and the time duration of "switch off" can be written as functions of v_n^*.

The function f_3 in (18.170) depends on v_n^*, as shown in (18.171). For each motion in (18.170), the time duration of "switch on" and the time duration of "switch off" can be written as functions of v_n^*

$$\begin{cases} t_{oni}(v_n^*) = \dfrac{\Delta}{\left\| f_{3i}(v_n^*) - \frac{U_{dc}}{3L} \right\|} \\ t_{offi}(v_n^*) = \dfrac{\Delta}{\left\| f_{3i}(v_n^*) + \frac{U_{dc}}{3L} \right\|} \end{cases} \tag{18.173}$$

It means that the switching frequency of the i-th motion is a function of v_n^* as well.

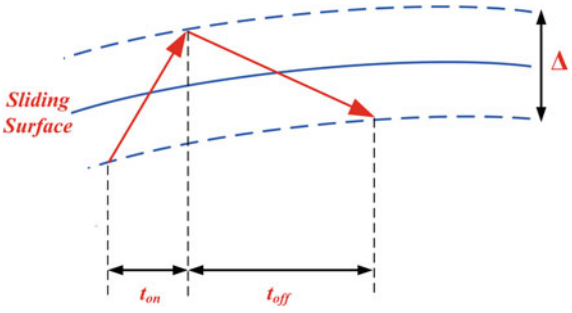

Fig. 18.35 Sliding manifold of SMPWM

$$f_{switch\_i}(v_n^*) = \frac{1}{t_{oni}(v_n^*) + t_{offi}(v_n^*)} \tag{18.174}$$

Taking into account all three motions in (18.170), the variable f_{switch} defined in (18.87) can be used as a measurement of the overall switching frequency of the system:

$$f_{switch\_i}(v_n^*) = \sum_{i=1}^{3} f_{switch\_i}(v_n^*) \tag{18.175}$$

Let $f_{switch\_i}(v_n^*)$ be the function to be minimized under the constraint $\frac{U_{dc}}{3L} > sup \| f_3 \|$. Then, the optimal v_n^* can be found from (18.172) and (18.173), such that $f_{switch\_i}(v_n^*)$ is minimized. In this particular example, the performance criterion is a function of v_n^*. In other problems, criterion could be a function of v_n. Then let v_n^* equal to the optimal value of v_n, and the tracking $v_n = v_n^*$ is provided by SMPWM.

Table 18.8 Simulation parameters of the three-phase AC/DC inverter

Parameter	U_{dc} (V)	$E_{abc,\ rms}$ (V)	$i^*_{abc,\ peak}$ (A)	R (Ω)	L (mH)	Step (μs)	Freq. (Hz)
Value	650	200	18	0.06	12	10	60

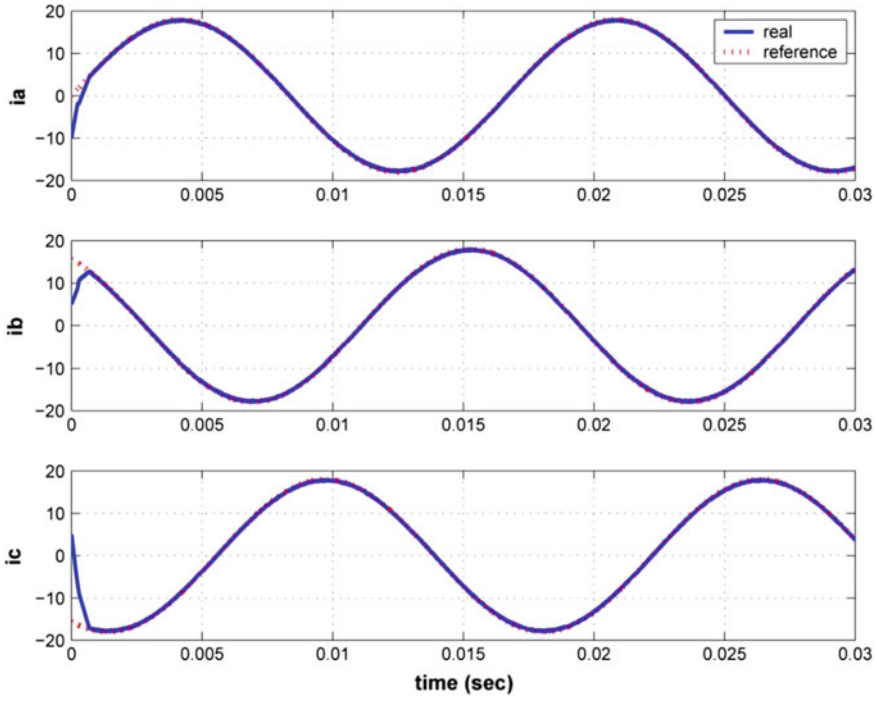

Fig. 18.36 Current tracking using SMPWM

18.4.5 Simulation Results

In order to evaluate the proposed control algorithm, computer simulations have been conducted using MATLAB/SIMULAINK software. Parameters used in simulation are listed in Table 18.8. This simulation used sliding surface decoupling approach. Results of three-phase current tracking (zoomed-in) are shown in Fig. 18.35. After the transient stage, phase currents track the references very well. Discontinuous output voltages v_a, v_b, v_c are shown in Fig. 18.36. In Fig. 18.37, the average value of v_n tracks a time varying reference. This average value is obtained by a first order dynamic $\mu\dot{x} = -x + v_n$ and $\mu = 0.001$. This low pass filter is used to calculate the average value of v_n in order to illustrate how close is this value to the v_n^*. Of course this filter is not needed for implementation of the system. In this simulation, the reference v_n^* is a randomly selected time varying function. It is not optimized according to some criterion. The only objective of Fig. 18.37 is to show the ability to track a time varying.

It is worth mentioning that SMPWM (see Fig. 18.38) is suitable for both analog and digital implementations. This due to the fact that SMPWM can be implemented with or without timing functionality, while other PWM approaches like Space Vector PWM require the DSP controller to have the ability to handle timing [7, 41].

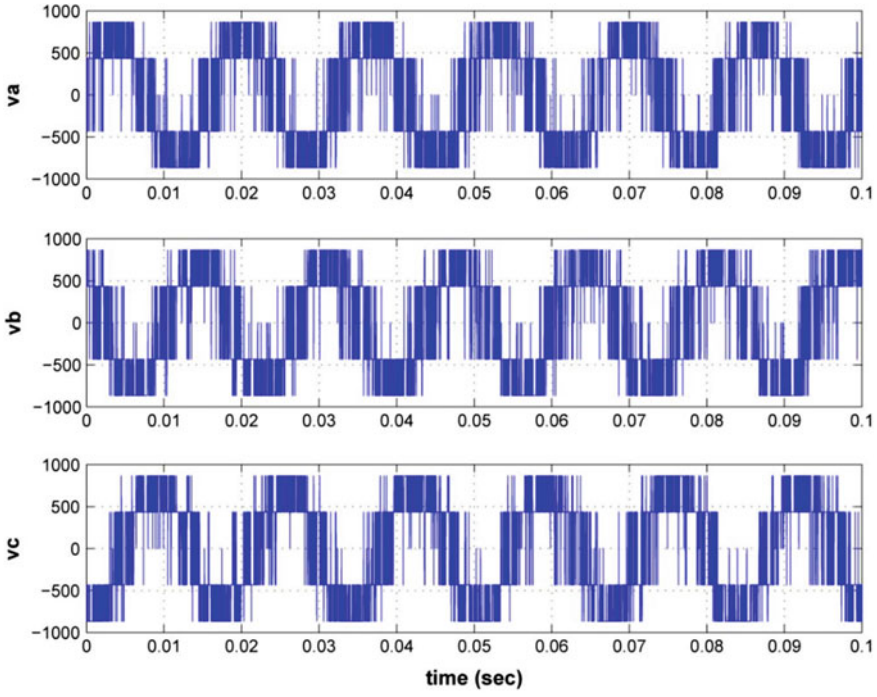

Fig. 18.37 Three-phase output voltages using SMPWM

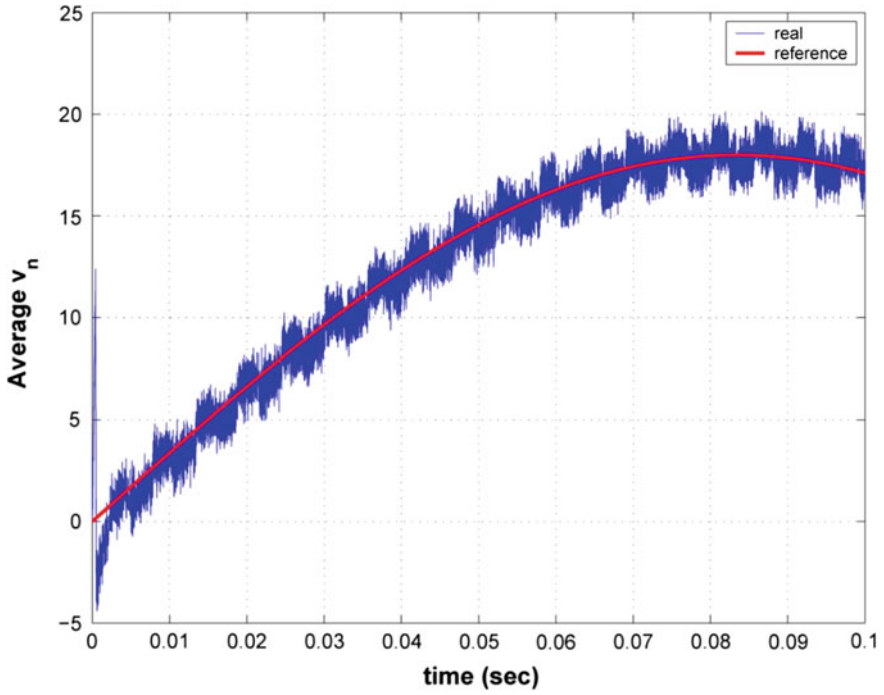

Fig. 18.38 Tracking a time varying $v_n^*(t)$ using SMPWM

References

1. Bartolini, G., Fridman, L., Pisano, A., Usai, E.: Modern Sliding Mode Control Theory: New Perspectives and Applications. Lecture Notes in Control and Information Sciences, vol. 375 (2008)
2. Biel, D., Fossas, E.: Some experiments on chattering suppression in power converters. In: Control Applications, (CCA) & Intelligent Control, (ISIC), 2009 IEEE, pp. 1523–1528. IEEE (2009)
3. Blasko, V.: Analysis of a hybrid pwm based on modified space-vector and triangle-comparison methods. IEEE Trans. Ind. Appl. **33**(3), 756–764 (1997)
4. Bondarev, A., Bondarev, S., Kostyleva, N., Utkin, V.I.: Sliding modes in systems with asymptotic state observers. Avtomatika i Telemekhanika **6**, 5–11 (1985)
5. Bowes, S.R., Clark, P.R.: Transputer-based harmonic-elimination pwm control of inverter drives. IEEE Trans. Ind. Appl. **28**(1), 72–80 (1992)
6. Bowes, S.R., Clark, P.R.: Regular-sampled harmonic-elimination pwm control of inverter drives. IEEE Trans. Power Electron. **10**(5), 521–531 (1995)
7. Chassaing, R.: DSP Applications Using C and the TMS320C6x DSK, vol. 13. Wiley, New York (2003)
8. Chen, L., Blaabjerg, F., Frederiksen, P.: An improved predictive control for three-phase pwm ac/dc converter with low sampling frequency. In: 20th International Conference on Industrial Electronics, Control and Instrumentation, 1994. IECON'94, vol. 1, pp. 399–404. IEEE (1994)

9. Cortes, D., Alvarez, J.: Robust sliding mode control for the boost converter. In: Power Electronics Congress, 2002. Technical Proceedings. CIEP 2002. VIII IEEE International, pp. 208–212. IEEE (2002)
10. DeCarlo, R.A., Zak, S.H., Matthews, G.P.: Variable structure control of nonlinear multivariable systems: a tutorial. Proc. IEEE **76**(3), 212–232 (1988)
11. Drakunov, S., Utkin, V., Zarei, S., Miller, J.: Sliding mode observers for automotive applications. In: Proceedings of the 1996 IEEE International Conference on Control Applications, 1996, pp. 344–346. IEEE (1996)
12. Drakunov, S.V., Izosimov, D., Lukyanov, A., Utkin, V., Utkin, V.: A hierarchical principle of the control systems decomposition based on motion separation. In: 9th IFAC Congress, vol. V, pp. 134–139 (1984)
13. Drakunov, S.V., Izosimov, D., Lukyanov, A., Utkin, V., Utkin, V.: Block control principle. ii. Autom. Remote Control **51**(6), 737–746 (1990)
14. Emelyanov, S., Utkin, V., Taran, V., Kostyleva, N., Shubladze, A., Ezerov, V., et al.: Theory of Variable Structure Systems. Nauka, Moscow (1970)
15. Habetler, T.G.: A space vector-based rectifier regulator for ac/dc/ac converters. IEEE Trans. Power Electron. **8**(1), 30–36 (1993)
16. Hashimoto, H., Utkin, V., Xu, J.X., Suzuki, H., Harashima, F.: Vss observer for linear time varying system. In: Industrial Electronics Society, 1990. IECON'90, 16th Annual Conference of IEEE, pp. 34–39. IEEE (1990)
17. Holtz, J., Lotzkat, W., Khambadkone, A.M.: On continuous control of pwm inverters in the overmodulation range including the six-step mode. IEEE Trans. Power Electron. **8**(4), 546–553 (1993)
18. Kazmierkowski, M.P., Dzieniakowski, M.A., Sulkowski, W.: Novel space vector based current controllers for pwm-inverters. IEEE Trans. Power Electron. **6**(1), 158–166 (1991)
19. Kokotović, P.V.: Applications of singular perturbation techniques to control problems. SIAM Rev. **26**(4), 501–550 (1984)
20. Kokotovic, P.V., O'malley, R., Sannuti, P.: Singular perturbations and order reduction in control theoryan overview. Automatica **12**(2), 123–132 (1976)
21. Komurcugil, H., Kukrer, O.: A novel current-control method for three-phase pwm ac/dc voltage-source converters. IEEE Trans. Ind. Electron. **46**(3), 544–553 (1999)
22. Krein, P.T.: Elements of Power Electronics, vol. 126. Oxford University Press, New York (1998)
23. Krstic, M., Kanellakopoulos, I., Kokotovic, P.V.: Nonlinear and Adaptive Control Design. Wiley, New York (1995)
24. Lee, H., Utkin, V.: Chattering analysis. Advances in Variable Structure and Sliding Mode Control. Lecture Notes in Control and Information Science, vol. 334, pp. 107–121. Springer, Berlin (2006)
25. Lukyanov, A., Utkin, V.: Methods of reducing equations for dynamic-systems to a regular form. Autom. Remote Control **42**(4), 413–420 (1981)
26. Martinez-Salamero, L., Cid-Pastor, A., Giral, R., Calvente, J., Utkin, V.: Why is sliding mode control methodology needed for power converters? In: Power Electronics and Motion Control Conference (EPE/PEMC), 2010 14th International, pp. S9–25. IEEE (2010)
27. Miwa, B.A., Otten, D.M., Schlecht, M.: High efficiency power factor correction using interleaving techniques. In: Applied Power Electronics Conference and Exposition, 1992. APEC'92. Conference Proceedings 1992., Seventh Annual, pp. 557–568. IEEE (1992)
28. Mohan, N., Undeland, T.M.: Power Electronics: Converters, Applications, and Design. Wiley, New York (2007)
29. Nguyen, V.M., Lee, C.: Tracking control of buck converter using sliding-mode with adaptive hysteresis. In: Power Electronics Specialists Conference, 1995. PESC'95 Record., 26th Annual IEEE, vol. 2, pp. 1086–1093. IEEE (1995)
30. Ooi, B.T., Dixon, J.W., Kulkarni, A.B., Nishimoto, M.: An integrated ac drive system using a controlled-current pwm rectifier/inverter link. In: Power Electronics Specialists Conference, 1986 17th Annual IEEE, pp. 494–501. IEEE (1986)
31. Rashid Muhammad, H.: Power Electronics Handbook. Academic Press, San Diego (2001)

32. Sira-Ramirez, H.: Sliding-mode control on slow manifolds of dc-to-dc power converters. Int. J. Control **47**(5), 1323–1340 (1988)
33. Sira-Ramírez, H.: Sliding Mode Control: The Delta-Sigma Modulation Approach. Birkhäuser (2015)
34. Sira-Ramirez, H., Escobar, G., Ortega, R.: On passivity-based sliding mode control of switched dc-to-dc power converters. In: IEEE Conference on Decision and Control, vol. 3, pp. 2525–2526. Institute Of Electrical Engineers Inc (IEE) (1996)
35. Sira-Ramírez, H., Silva-Ortigoza, R.: Control Design Techniques in Power Electronics Devices. Springer Science & Business Media, London (2006)
36. Slotine, J.J.E.: Sliding controller design for non-linear systems. Int. J. Control **40**(2), 421–434 (1984)
37. Trzynadlowski, A.M., Wang, Z., Nagashima, J.M., Stancu, C., Zelechowski, M.H.: Comparative investigation of pwm techniques for a new drive for electric vehicles. IEEE Trans. Ind. Appl. **39**(5), 1396–1403 (2003)
38. Utkin, V.: Sliding Modes in Control and Optimization. Springer, Berlin (1992)
39. Utkin, V., Guldner, J., Shi, J.: Sliding Mode Control in Electro-mechanical Systems, vol. 34. CRC Press, Boca Raton (2009)
40. Utkin, V.I.: Sliding Modes and Their Application in Variable Structure Systems. Mir publishers, Moscow (1978)
41. van Der Broeck, H.W., Skudelny, H.C., Stanke, G.V.: Analysis and realization of a pulsewidth modulator based on voltage space vectors. IEEE Trans. Ind. Appl. **24**(1), 142–150 (1988)
42. Utkin, V.I., Chen, D.S., Zarei, S., Miller, J.: Discrete time sliding mode observer for automotive alternator. In: Control Conference (ECC), 1997 European, pp. 3025–3030. IEEE (1997)
43. Venkataramanan, R., Sabanovic, A., Cuk, S.: Sliding mode control of dc-to-dc converters. In: Proceedings, IEEE Conference on Industrial Electronics, Control and Instrumentations (IECON), pp. 251–258 (1985)
44. Wong, C., Mohan, N., He, J.: Adaptive phase control for three phase pwm ac-to-dc converters with constant switching frequency. In: Conference Record of the Power Conversion Conference, 1993. Yokohama 1993, pp. 73–78. IEEE (1993)
45. Woo, W., Lee, N., Schuellein, G.: Multi-phase buck converter design with two-phase coupled inductors, applied power electronics conference and exposition, 2006. In: APEC, vol. 6, p. 6 (2006)
46. Wu, R., Dewan, S.B., Slemon, G.R.: A pwm ac-to-dc converter with fixed switching frequency. IEEE Trans. Ind. Appl. **26**(5), 880–885 (1990)
47. Wu, R., Dewan, S.B., Slemon, G.R.: Analysis of an ac-to-dc voltage source converter using pwm with phase and amplitude control. IEEE Trans. Ind. Appl. **27**(2), 355–364 (1991)
48. Xu, P., Wei, J., Lee, F.C.: Multiphase coupled-buck converter-a novel high efficient 12 v voltage regulator module. IEEE Trans. Power Electron. **18**(1), 74–82 (2003)